ZMPSTE24 Missense Mutations that Cause Progeroid Diseases Decrease Prelamin A Cleavage Activity, Protein Stability, or Both

Eric D. Spear[1], Ehr Ting Hsu[2], Laiyin Nie[3], Elisabeth P. Carpenter[3], Christine A. Hrycyna[2], Susan Michaelis[1]*

[1]Department of Cell Biology, The Johns Hopkins School of Medicine, Baltimore, MD 21205
[2]Department of Chemistry, Purdue University, West Lafayette, IN 47907
[3]Structural Genomics Consortium, University of Oxford, Oxford, UK

*Corresponding author:
Susan Michaelis
Dept. of Cell Biology
725 N. Wolfe St.
Baltimore, MD 21205
Phone: 410-955-7274
E-mail: Michaelis@jhmi.edu

ABSTRACT

The human zinc metalloprotease ZMPSTE24 is an integral membrane protein critical for the final step in the biogenesis of the nuclear scaffold protein lamin A, encoded by *LMNA*. After farnesylation and carboxyl methylation of its C-terminal CAAX motif, the lamin A precursor, prelamin A, undergoes proteolytic removal of its modified C-terminal 15 amino acids by ZMPSTE24. Mutations in *LMNA* or *ZMPSTE24* that impede prelamin A cleavage cause the premature aging disease Hutchinson-Gilford Progeria Syndrome (HGPS) and the related progeroid disorders, mandibuloacral dysplasia type B (MAD-B), and restrictive dermopathy (RD). Here we report a "humanized yeast" system to assay ZMPSTE24-dependent cleavage of prelamin A and examine the eight known disease-associated *ZMPSTE24* missense mutations. All show diminished prelamin A processing and fall into three classes, with defects in activity (Class I), protein stability (Class II), or both (Class III). Class II ZMPSTE24 mutants can be rescued by deleting the E3 ubiquitin ligase Doa10, involved in ER-associated protein degradation of misfolded membrane proteins, which may have therapeutic implications. We also show that ZMPSTE24-mediated prelamin A cleavage can be uncoupled from the recently discovered role of ZMPSTE24 in the clearance of ER membrane translocon-clogged substrates. Together with the crystal structure of ZMPSTE24, this "humanized yeast system" can guide structure-function studies to uncover the mechanisms of prelamin A cleavage, translocon unclogging, and membrane protein folding and stability.

INTRODUCTION

The integral membrane zinc metalloprotease ZMPSTE24 plays a critical role in human health and longevity through its role in the maturation of the nuclear scaffold protein lamin A from its precursor, prelamin A (1-3). Mature lamin A, together with nuclear lamins B and C, contributes to the structural integrity and proper functioning of the nucleus (4-10). Defects in prelamin A processing by ZMPSTE24 are a primary cause of progeria (2,11-13). The premature aging disorder Hutchinson-Gilford Progeria syndrome (HGPS; OMIM #176670) results from mutations in the *LMNA* gene (encoding prelamin A) that block ZMPSTE24 processing, while the related progeroid diseases mandibuloacral dysplasia-type B (MAD-B; OMIM #608612) and restrictive dermopathy (RD; OMIM #275210) result from *ZMPSTE24* mutations that diminish protease function (12,14-16). Understanding the mechanistic details of prelamin A processing by ZMPSTE24 is thus critical for designing therapeutic approaches for these progeroid diseases and may also provide insights into the normal physiological aging process.

The posttranslational maturation of prelamin A is a multi-step process. Prelamin A contains a C-terminal CAAX motif (C is cysteine, A is usually an aliphatic amino acid, and X is any residue). Like other CAAX proteins, prelamin A undergoes a series of three reactions, referred to as CAAX processing (Fig. 1, Steps 1-3) which includes farnesylation of cysteine, proteolytic removal of the -AAX residues mediated redundantly by ZMPSTE24 or RCE1, and carboxyl methylation of the farnesylated cysteine (2,12,17,18). Prelamin A is distinct from all other CAAX proteins in higher eukaryotes in that following CAAX processing, prelamin A undergoes a second endoproteolytic cleavage event uniquely mediated by ZMPSTE24 (Fig. 1, Step 4). This second cleavage removes the C-terminal 15 amino acids, including the modified cysteine, to yield mature lamin A (1,3). In progeroid disorders, this second ZMPSTE24-promoted cleavage of prelamin A is compromised, leading to the accumulation of a permanently farnesylated and carboxyl methylated form of prelamin A, which is the toxic “culprit” in disease (12,13,19).

MAD-B, HGPS, and RD represent a spectrum of disorders of increasing severity (16,20). In HGPS, the best studied of these, children manifest accelerated aging symptoms starting at one year of age, including failure to thrive, lipodystrophy, hair loss, joint ailments, and cardiovascular disease, and they typically die in their mid-teens from heart attack or stroke. Nearly all HGPS patients harbor a dominant *LMNA* mutation that, through altered splicing, generates an internally deleted version of prelamin A called progerin, which retains its CAAX motif but lacks the ZMPSTE24 cleavage site, and causes disease phenotypes (13-15,21). RD and MAD-B are due to recessive mutations in *ZMPSTE24*, and result from the accumulation of full-length prelamin A that

is permanently farnesylated and carboxyl methylated. RD is far more severe than HGPS, being fatal at or before birth, and is due to complete loss of ZMPSTE24 function resulting from null mutations (frameshifts, premature termination, or large deletions) in both copies of *ZMPSTE24* (16,22-24). In contrast, MAD-B is generally milder than HGPS, with patients having variable survival rates and disease severity, yet all exhibiting lipodystrophy as a major disease phenotype. Individuals with MAD-B have one *ZMPSTE24* null allele and one *ZMPSTE24* missense allele that provides reduced but residual function (Table 1) (16,20,25). In general, the severity of these three progeroid diseases reflects the amount of permanently farnesylated and carboxyl methylated prelamin A that accumulates per cell. Recently individuals with metabolic syndrome and nonalchoholic fatty liver disease (NAFLD), both lipodystrophy-associated disorders, were also found to have a *ZMPSTE24* missense mutation (Table 1) (26-28). In addition, diminished ZMPSTE24 processing of prelamin A may be important in normal aging, based on a study showing that prelamin A accumulation occurs in blood vessels from aging, and not young, individuals (29). Because of the importance of diminished ZMPSTE24 processing of prelamin A in progeroid disease and possibly during normal aging, understanding the detailed mechanism of ZMPSTE24 is an important area of research.

ZMPSTE24 is widely conserved in eukaryotes ranging from yeast to mammals (30-32). The *Saccharomyces cerevisiae* homolog Ste24 is the founding member of this family and was discovered based on its role in the proteolytic maturation of the secreted yeast mating pheromone a-factor (17,33-36). Prelamin A and the a-factor precursor are distinct from other CAAX proteins, as they are the only ones that undergo additional cleavage by ZMPSTE24/Ste24 after CAAX processing is completed (1,3,33,37,38). ZMPSTE24 and its homologs contain seven transmembrane spans and a consensus zinc metalloprotease HEXXH motif (H is histidine, E is glutamate, X is any amino acid) which is critical for coordinating zinc and performing catalysis (20,32). The recently solved X-ray crystallography structure of human ZMPSTE24, and that of the virtually superimposable yeast Ste24, reveal it to be a completely novel class of protease (31,32,39). The seven helical spans of ZMPSTE24 form a voluminous intramembrane “hollow” chamber, with the HEXXH catalytic domain positioned such that it faces the interior of the chamber, with a side portal(s) in the chamber presumably providing a site for prelamin A entry. This unusual ZMPSTE24 structure raises important functional questions, including how ZMPSTE24 mediates specificity for prelamin A access into its chamber, what residues are involved in positioning prelamin A for its cleavage(s), and what might be the role of ZMPSTE24’s large chamber. The answers to these questions are of fundamental biological interest and will help us to understand how specific ZMPSTE24 disease alleles malfunction and might be corrected. They may also shed

light on how certain HIV protease inhibitors such as lopinavir are able to inhibit ZMPSTE24 (40,41). Such insights could also have relevance to physiological aging.

ZMPSTE24 is dually localized in the inner nuclear and ER membranes (42) and performs cellular functions in addition to its well-established role in the proteolytic maturation of prelamin A and a-factor. Recent work shows that ZMPSTE24 plays a protein quality control role by clearing "clogged" Sec61 translocons of post-translationally secreted proteins that have aberrantly folded while in the process of translocation (43). Intriguingly, a role for ZMPSTE24 in defending cells against a wide variety of enveloped viruses, independent of its catalytic activity, has also been recently reported (44).

Because of ZMPSTE24's importance in human health and disease and its novel structure, it would be advantageous have a high throughput system to probe structure-function relationships in this protease. Here we report a "humanized yeast system" to specifically assay the second ZMPSTE24 cleavage step in prelamin A maturation (Fig. 1, Step 4). We show that the eight currently known disease-causing ZMPSTE24 missense alleles (Table 1) all have decreased prelamin A cleavage *in vivo* and fall into distinct classes- those that affect solely catalysis, those that affect *in vivo* protein stability through ER-associated degradation (ERAD) by the ubiquitin-proteasome system (UPS), and those that affect both. Notably, for two unstable ZMPSTE24 disease mutants, P248L and W340R, when ubiquitylation is blocked by deletion of the yeast gene encoding the E3 ligase *DOA10*, both their stability and catalytic activity are significantly restored, which has implications for therapeutic strategies that could ultimately optimize "personalized medicine" approaches. The *in vivo* assay system we present here, along with the ease of gene manipulation and genetic strategies available in yeast, hold promise for future high-throughput structure-function studies on ZMPSTE24.

RESULTS

ZMPSTE24 can perform the upstream cleavage of its *bona fide* substrate prelamin A in yeast

We previously showed that human ZMPSTE24 could functionally replace its yeast homolog Ste24 for the proteolytic maturation of its non-native substrate, the yeast mating pheromone a-factor (30,36,45). We also developed an assay in which the extent of yeast mating broadly correlated with the severity of ZMPSTE24 disease alleles, such that those that cause RD (null alleles) show more severe mating defects than those that cause the milder disease MAD-B (missense alleles) (20). However, the mating assay is less than ideal for the mechanistic dissection of ZMPSTE24 because it relies on ZMPSTE24-dependent cleavage of the cross-species substrate a-factor, and because it cannot distinguish between ZMPSTE24's two cleavage activities. Because the unique step in prelamin A cleavage by ZMPSTE24 is the second cleavage, and because it is the lack of this step that causes progeroid diseases, we set out to develop a system to specifically measure this ZMPSTE24-mediated processing step for its *bona fide* substrate prelamin A, which is not normally present in *S. cerevisiae*.

To create a 'humanized' yeast system to study ZMPSTE24-dependent processing of prelamin A, we expressed a C-terminal segment from the human prelamin A protein (amino acids 431-664) (Fig. 2A), which contains all the necessary signals for CAAX processing and the ZMPSTE24-dependent unique cleavage (42,46). To serve as size markers for comparison, we also constructed a mutant prelamin A, L647R, that is known to be uncleavable by ZMPSTE24 in mammalian cells (46-49) as well as a version expressing the correctly processed mature form of prelamin A (amino acids 431-646). All versions were N-terminally tagged with 10His-3myc to allow detection by western blotting and were integrated into the yeast chromosome at the *HO* locus. In this humanized yeast system ZMPSTE24 is expressed from a low-copy number yeast Cen plasmid and prelamin A cleavage is measured by quantitation of the mature and prelamin A species present in cells at steady state. Importantly, our strain background retains Rce1 to allow efficient –AAXing (Fig. 1, Step2), thus eliminating any effect that mutant ZMPSTE24 proteins may have on this first cleavage step.

We first tested whether human ZMPSTE24 could process prelamin A in a *ste24*Δ strain. Plasmid-borne ZMPSTE24, but not vector alone, resulted in two bands observed by western blotting (Fig. 2B, compare lanes 1 and 2). Importantly, these bands co-migrated with the "uncleavable" and "mature" forms (Fig. 2B, lanes 3 and 4, respectively), indicating that the prelamin A substrate was properly cleaved by ZMPSTE24. We note that yeast Ste24 can also cleave

prelamin A (Fig. S1) and that prelamin A processing to the mature form by ZMPSTE24 is 75-80% complete in this system and can be further boosted by the addition of a second copy of ZMPSTE24 (Fig. S2).

We also tested whether prelamin A cleavage in yeast required the CAAX modifications farnesylation and carboxyl methylation, as it does in mammalian cells (42,46). Wild-type ZMPSTE24, but not a catalytic-dead mutant, H335A, resulted in mostly mature lamin A (Fig. 3A, compare lanes 1 and 2). Mutation of the CAAX motif cysteine to a serine (C661S), which prevents its farnesylation, completely blocked ZMPSTE24-dependent cleavage of prelamin A (Fig. 3A, lane 3). The unmodified C661S prelamin A migrated slightly more slowly than farnesylated prelamin A in the H335A ZMPSTE24 mutant (Fig. 3A, compare lanes 2 and 3), as has been previously observed (50). We also examined prelamin A cleavage in a *ste14*Δ strain, which lacks the yeast ICMT. As observed in mammalian cells (42,46,51), blocking carboxyl methylation of the prelamin A substrate has a modest, but discernable effect on prelamin A cleavage (Fig. 3B, compare lane 3 to lane 1). Taken together, these experiments demonstrate the processing of prelamin A in yeast follows the same rules as in mammalian cells. Thus we can use our "humanized" yeast system to study ZMPSTE24-dependent processing of its *bona fide* substrate prelamin A.

All ZMPSTE24 disease missense mutations show reduced prelamin A cleavage and some exhibit a low level of protein

One goal of developing a yeast *in vivo* cleavage assay was to determine whether particular *ZMPSTE24* disease alleles resulted in defective prelamin A cleavage, and by what mechanism(s), which ultimately might suggest therapeutic possibilities. Currently, eight different ZMPSTE24 substitution mutations are known to cause progeroid disorders (Table 1). We examined the processing efficiency of these alleles compared to WT ZMPSTE24. Also included in our panel are two mutations, H335A and H339A, known to abolish ZMPSTE24 activity by disrupting the zinc metalloprotease domain ($H_{335}EXXH_{339}$) (20,30,32,35). As evident in Fig. 4A and summarized in Table 2, all of the mutations we examined showed reduced *in vivo* prelamin A cleavage compared to wild-type ZMPSTE24, albeit to widely varying degrees. For instance, L438F shows that highest residual activity at 57.2% that of WT ZMPSTE24, while L462R shows the least at 6.5% (Fig. 4A, compare lanes 11 and 12 to lane 2). Notably none of the disease alleles are as severe as the two catalytic dead mutants H335A and H339A (Fig. 4A, lanes 6 and 7) which have <2% WT ZMPSTE24 activity. Some of the mutations in our panel were previously shown to accumulate prelamin A in patient cells (L94P, P248L, N265S, L425P, and L438F; (27,52-55)), but directly comparing the extent of severity for these *ZMPSTE24* alleles was not possible in non-isogenic

patient cells. The yeast system, however, is ideal for this purpose. Three of the mutants, W340R, Y399C, and L462R, had never been examined for prelamin A processing defects. Thus, our yeast system has for the first time confirmed the molecular basis underlying these latter mutants (prelamin A accumulation) and allows us to compare levels of residual processing between all known ZMPSTE24 disease alleles.

Given the non-conservative amino acid substitutions in several of the ZMPSTE24 mutants, we considered the possibility that decreased prelamin A cleavage could at least in part be the result of ZMPSTE24 misfolding and subsequent degradation. Indeed, four of the mutants (L94P, P248L, W340R and L462R) showed steady-state ZMPSTE24 levels significantly less (<40%) than that of wild-type ZMPSTE24 (Fig. 4B, compare lanes 3, 4, 8 and 12 to lane 2). Notably, when we calculated the "adjusted ZMPSTE24 activity" (Table 2), in which the efficiency of prelamin A processing is corrected for the amount of ZMPSTE24 protein present, the value of two of these mutants, P248L and W340R, is 100% or higher, suggesting that degradation, and not compromised catalytic activity, are the problem for theses alleles (indeed, in the section below, we find these two mutants are fully active when their degradation is blocked). Strikingly, however, other mutants, including N265S and Y399C, displayed near-normal ZMPSTE24 protein levels, yet retained only ~25-30% activity (Fig. 4A and B), which albeit less than WT, is far more than that of the catalytic dead mutants H335A, H339A (<2%) (Table 2).

Together, these results demonstrate that the humanized yeast system can differentiate three classes of ZMPSTE24 disease mutations: Class I mutants are those that affect mainly enzymatic activity (N265S and Y399C), Class II are those that affect mainly protein stability (P248L, W340R), and Class III are those that appear to affect both (L94P, L425P, L438F, and L462R).

Blocking ubiquitylation and degradation of the ZMPSTE24 disease mutants rescues the prelamin A cleavage defect

Mutations in transmembrane proteins like ZMPSTE24 can result in degradation by the UPS, causing disease despite the fact that their catalytic function remains intact. In some cases, enhancing the folding or blocking the degradation of these mutant proteins using pharmacological chaperones, proteasome inhibitors, or mutants defective in ubiquitiylation, can rescue protein levels enough to restore function within the cell (56-58). We therefore asked whether blocking the ubiquitylation of the most unstable ZMPSTE24 mutant proteins, L94P, P248L, W340R and L462R, could rescue prelamin A cleavage.

To do this we used a *doa10*Δ mutant, which lacks the key yeast E3 ubiquitin ligase, Doa10,

that mediates the ubiquitylation and subsequent degradation of many misfolded transmembrane proteins (59,60). Steady-state levels of all of these unstable ZMPSTE24 mutant proteins increase ~2-5 fold in the *doa10*Δ strain, indicating all are substrates, either partially or fully, of this ubiquitin ligase (Fig. 5A, compare adjacent lanes for each disease mutant). Interestingly, we observed that stabilization of P248L and W340R in the *doa10*Δ strain, but not L94P or L462R, restored prelamin A cleavage activity to near wild-type levels (Fig. 5B, compare adjacent lanes 5 and 6, 7 and 8, versus 3 and 4, 9 and 10) . Notably, these same two mutants, P248L and W340R, had shown WT or better "adjusted ZMPSTE24 activity" above (Table 2), when activity was normalized to the amount of ZMPSTE24 protein present. We also tested whether the proteasome inhibitor bortezamib had similar effects as the *doa10*Δ mutant (Fig. S3). Although we observed stabilization of unstable ZMPSTE24 mutants, prelamin A cleavage was not dramatically improved for any ZMPSTE24 mutant tested, possibly because stabilization was not maximal in this test or ubiquitylation of ZMPSTE24 interferes with its catalytic activity.

Taken together, these data suggest that some ZMPSTE24 patient mutations (Class II) are prematurely targeted for ubiquitin-mediated degradation, despite retaining catalytic activity. For these alleles, therapeutic strategies could be developed that reverse the destruction of these otherwise functional enzymes by blocking their ubiquitylation.

The prelamin A cleavage and Sec61 translocon clearance functions of ZMPSTE24 can be genetically separated

Recently, yeast Ste24 and mammalian ZMPSTE24 were shown to have a specialized protein quality role for handling postranslationally secreted proteins that prematurely fold while translocating across the ER membrane, thereby "clogging" the Sec61 translocation machinery (43). Clearance of a reporter "clogger" protein by yeast Ste24 or heterologously expressed human ZMPSTE24 in *ste24*Δ yeast cells were shown to require their catalytic activity. Although four ZMPSTE24 disease alleles, including L94P, P248L, W340R and L438F, were previously assayed for their ability to clear the clogger substrate and shown to be defective to varying extents (43), four additional mutants in our current study were not tested.

The "clogger" reporter is a chimeric protein composed of the yeast glycoprotein Pdi1 fused to the clogging element bacterial dihydrofolate reductase (DHFR), followed by a stretch of N-linked glycosylation sequences. Its complete translocation into the ER lumen is observed as an SDS-PAGE mobility shift when all N-glycosylation sites (in both Pdi1 and the C-terminus) are modified. The hemi-glycosylated substrate is assumed to be partially translocated (clogged) and the unmodified protein represents a cytoplasmic pool that accumulates upon translocon clogging (Fig.

6). As observed previously, *ste24*Δ cells transformed with vector alone or the catalytic-dead ZMPSTE24 variants H335A and H339A had the most severe defects (Fig. 6, lanes 1, 6 and 7, respectively), with 36-44% of the reporter accumulating in the "clogged/cytoplasmic" form, compared to only ~18% for wild-type ZMPSTE24 (Fig. 6, lane 2). Likewise, L94P and P248L, which have severe prelamin A processing defects also showed significant "clogged/cytoplasmic" accumulation (~30%) (Fig. 6, lanes 3 and 4) and W340R showed a modest but discernable effect (Fig. 6, lane 8). Surprisingly, however, other ZMPSTE24 mutants, including Y399C, L425P, L438F and L462R, despite showing strong prelamin A cleavage defects, had little to no defects in "clogger" clearance (Fig. 6, lanes 5 and 9-12). L462R is particularly notable as it is relatively unstable and has a strong prelamin A cleavage defect, yet is largely proficient in clogger clearance. In addition, Y399C is the most stable ZMPSTE24 mutant we examined, but also displays a dichotomy in prelamin A cleavage and de-clogging activities. These findings suggest that while catalytic activity is required for both of ZMPSTE24's functions, prelamin A processing and "declogging" may differ in important ways mechanistically. For instance, mutant ZMPSTE24 proteins may be differently affected in their ability to be recruited to the Sec61 translocon, or in their ability to permit access of the two different types of substrates (prelamin A *vs*. clogged proteins) into their active site chamber. It will be of interest to attempt to isolate ZMPSTE24 variants that can efficiently process prelamin A, but are defective for clogger clearance.

DISCUSSION

A "humanized yeast system" for analysis of ZMPSTE24 cleavage of prelamin A.

Gaining an understanding of how the structure of a protein dictates its function is facilitated by assaying the impact of specific mutations on activity, protein stability, and interactions *in vivo*. For proteins involved in disease, this information can also provide invaluable insights into personalized medicine strategies, as exemplified by the customized therapies recently developed to treat cystic fibrosis patients with different disease alleles of the *CFTR* gene (56). Here we report the development of an *in vivo* "humanized yeast" assay system to determine the impact of *ZMPSTE24* disease mutations on the cleavage of prelamin A (Fig. 1, Step 4), the step that is defective in progeroid diseases. Importantly, this yeast system allows us to measure both ZMPSTE24 prelamin A cleavage activity and *in vivo* protein stability, and has the potential to ultimately be scaled up for high throughput analysis of a large number of mutant alleles. Our humanized yeast system retains all of the known requirements observed in mammalian cells (Figs. 2 and 3) in that the prelamin A substrate must be farnesylated and carboxyl methylated for efficient cleavage, and mutation of a residue adjacent to the cleavage site in prelamin A (L647R) abolished processing in yeast, as it does in mammalian cells. Furthermore, mutation of the ZMPSTE24 catalytic motif HEHHX completely blocks prelamin A processing.

We previously used yeast to gain insight into *ZMPSTE24* disease alleles, based on the ability of human ZMPSTE24 to mediate the post-translational maturation of a non-native substrate, the yeast mating pheromone a-factor (20). In that study, yeast mating efficiency was measured as a proxy for directly assessing substrate cleavage. We showed that RD null alleles were completely devoid of mating, whereas the five ZMPSTE24 MAD-B missense mutations tested all showed some residual mating activity. That study supported the notion that even a small amount of ZMPSTE24 function diminishes disease severity and is beneficial for patients. However in that system it was not possible to determine whether –AAXing (Fig. 1 Step 2), the final cleavage step (Fig. 1, Step 4), or both were affected, since, in the absence of *RCE1*, both of these a-factor processing events were dependent on ZMPSTE24. In the current study, we have developed an improved and completely "humanized yeast" system (both substrate end enzyme are encoded by the human genes). And because *RCE1* is present, we can specifically examine the final prelamin A cleavage step mediated by ZMPSTE24. Thus, this optimized system permits assaying human ZMPSTE24's ability to cleave its *bona fide* substrate, human prelamin A, and cleavage is the direct output that is measured. The ease of this assay allows it to be significantly scaled up for the analysis of large numbers of mutants in the future.

ZMPSTE24 missense disease alleles show reduced prelamin A cleavage *in vivo* and define three mutant classes.

We tested all eight of the currently known *ZMPSTE24* missense alleles implicated in progeroid diseases (Table 1), along with two catalytic dead alleles that alter the HEXXH domain (H335A and H339A). While all of the disease mutants exhibit decreased overall prelamin A cleavage compared to wild-type *ZMPSTE24,* all show residual prelamin A cleavage activity, significantly greater than the catalytic dead allele (Fig. 4 and Table 2). However the mutants vary greatly in the extent of remaining activity (from 6%-57% that of WT). Importantly, four of the ZMPSTE24 mutations (L94P, P248L, W340R and L462R) showed marked decreases in ZMPSTE24 protein levels (14% - 40% of the WT level), suggesting they cause misfolding and subsequent degradation, while for the others, protein stability is only minimally affected. Taking into account both their activity and stability we can divide ZMPSTE24 disease alleles into 3 classes (Table 2): Class I mutations affect mainly cleavage activity (N265S and Y399C), Class II affect mainly protein stability (P248L, W340R), and Class III mutants affect both (L94P, L425P, L438F, and L462R).

For the highly unstable mutant proteins (L94P, P248L, W340R and L462R), the UPS is largely responsible for their degradation, since their ZMPSTE24 protein levels are significantly restored when cells are treated with the proteasome inhibitor Bortezomib, or when expressed in a *doa10*Δ strain (Figs. 5 and S4). *DOA10* encodes a dually localized ER and inner nuclear membrane E3 ligase known to ubiquitylate misfolded membrane proteins (59-61). Quite notably, for the P248L and W340R (Class II) mutants, but not for the L94P and L462R (Class III) mutants, prelamin A cleavage is dramatically restored to WT levels in the *doa10*Δ strain. This finding confirms the conclusion that the enzyme function of these two Class II mutant proteins remains largely intact, as also indicated by the “adjusted ZMPSTE24 activity” column in Table 2, despite the presence of mutations that target them for degradation, presumably due to misfolding. Indeed, preliminary experiments using purified ZMPSTE24 proteins show that the P248L and W340R variants retain significant prelamin A cleavage activity *in vitro* (L. Carpenter and L. Nie, unpublished observations). P248L was also suggested to retain significant activity in a previous study based on a-factor production (54). It should be noted Bortezomib treatment did not rescue prelamin A cleavage for P248L and W340R, despite partial rescue of protein levels (Fig S3). While this may reflect a technical aspect with our experimental methods, it is also possible that ubiquitin-modified ZMPSTE24, although accumulated in the cell, may lose enzymatic activity due to interference by ubiquitin. In the future, it will be of great interest to determine whether ZMPSTE24 protein levels and prelamin A processing can be restored in P248L and W340R disease patient

cells by genetic or chemical manipulations of the UPS. Such a finding could point the way to personalized medicine approaches that would differ between patients with Class II mutations and patients with Class I and III mutations that impact protein function. Although not yet directly tested in clinical trials, all patients with mutated versions of ZMPSTE24 are predicted to benefit from farnesyltransferase inhibitors (FTIs), which should render full-length prelamin A unmodified and thus less harmful, as it does for progerin in HGPS (13). However patients with Class II *ZMPSTE24* mutations could potentially improve even more by a combination of FTIs and UPS inhibitors.

Analysis of genetic dominance for L462R and L438F ZMPSTE24 alleles

Genetic pedigree analysis as well as patient genotypes indicates that generally *ZMPSTE24* mutations are recessive. Thus, disease is usually not manifest in individuals if one of their two *ZMPSTE24* alleles is WT. However two patient mutations, L462R and L438F, have been suggested to be exceptions and could be dominant, since mutations in the second *ZMPSTE24* allele were not identified in these patients by sequence analysis of exons (Table 1). These patients have RD and metabolic syndrome, respectively. Surprisingly however, the healthy mother of the L462R RD patient shared the same apparent genotype ($ZMPSTE24^{+/L462}$) as her affected offspring, arguing against dominance (62). We propose that L462R is actually recessive and that an as-yet-undetected mutation either inside (and missed, as has previously happened (23)) or outside the coding region (e.g. promoter, intron, etc.) may inactivate the second seemingly WT *ZMPSTE24* allele of the child with RD. A similar explanation may account for disease in L438F patients as well. Supporting this hypothesis and arguing against dominance, we found that an additional wild-type copy of *ZMPSTE24* could efficiently suppress the prelamin A cleavage defect observed in all *ZMPSTE24* disease alleles, including L462R as well as L438F (Fig. S4).

In light of the possibility that both L462R and L438F are actually recessive, an additional aspect of these mutations deserves mention. Most *ZMPSTE24* missense mutations cause MAD-B (Table 1). However, It is notable that we found that L462R is the “strongest” of the alleles studied here, showing significant residual activity, while L438F is the “weakest” (Fig. 4 and Table 2), which may explain why the former leads to the disease RD which is more severe than MAD-B, while the latter leads to metabolic disorder or NAFLD, diseases that are milder than MAD-B (26-28).

Some, but not all, disease alleles affect ZMPSTE24’s ability to clear clogged translocons

Our studies here suggest that the recently reported role for ZMPSTE24 in clearance of clogged translocons relies on certain features of the protease that may be separable from those required for prelamin A cleavage. As shown previously (43), wild-type ZMPSTE24, but not

catalytic-dead versions, can efficiently replace yeast Ste24 when challenged with a clogging-prone substrate (Fig. 6). Interestingly, we also show here that some mutants, including Y399C and L462R, show poor prelamin A processing (~25% and 6% of WT, respectively), yet are largely proficient in the unclogging process, while other mutants, including L94P and P248L, like the catalytic dead mutants, are defective in both processes. It is perhaps not surprising that the two different types of substrates (prelamin A and clogged proteins) might be handled differently. For instance, various ZMPSTE24 mutant proteins may differ in their ability to be recruited to the Sec61 translocon, or in their ability to permit access of the two different types of substrates to the active site. We speculate that like the Sec61 translocon itself, which is known to open laterally to release transmembrane spans (63-65), ZMPSTE24 may also have the capacity to do so to facilitate transfer of a clogged substrate from the translocon pore to the ZMPSTE24 protease catalytic site. Isolating more mutants specific to each function could help reveal important aspects about these processes. To date we have not searched for ZMPSTE24 mutants that remain fully active in prelamin A processing, but defective for clearance of a clogged protein, but such mutants could be sought using our yeast system and would provide further evidence that these activities are separable.

Utility of our humanized yeast system for structure-function analysis of ZMPSTE24

ZMPSTE24 is an intriguing molecule in terms of basic membrane protein biology, in addition to its importance for understanding progeroid diseases and physiological aging. While ZMPSTE24 has a canonical HEXXH zinc binding motif that can coordinate zinc and mediates catalysis, the ZMPST24 structure is fundamentally different from other proteases, because catalysis occurs within an unusual enclosed intramembrane chamber (31,32,39). This novel structure elicits a number of questions concerning ZMPSTE24 enzyme mechanism, prelamin A access and positioning, and why prelamin A is the sole specific substrate known for ZMPSTE24. As a starting point here, we focused here on the eight known ZMPSTE24 missense disease alleles. Six of the eight ZMPSTE24 disease alleles lie in residues highly conserved in ZMPSTE24/Ste24 among diverse species (the exceptions are L94 and Y399) and they cluster in two regions of the ZMPSTE24 structure (Fig. 7). Most are at the top of the chamber, near the HEXXH catalytic motif, which coordinates the zinc ion (yellow). It has been suggested that these mutations could affect catalysis directly (N265S), impede substrate binding (L438F and L462R), or substrate entry into the chamber (P248L and W430R) (32). Notably two mutations L94P and Y399C map to the bottom side of the chamber, suggesting a functionally important activity in that region of ZMPSTE24, possibly in farnesyl binding for proper substrate positioning. As discussed above, an important finding here is that some of disease mutations mainly produce an effect by destabilizing the protein,

rather than affecting its enzymatic function *per se*.

In the long term, we expect that the humanized yeast system reported here, along with high throughput mutagenesis, will allow us to answer mechanistic questions about how ZMPSTE24 functions and which features of misfolded versions of ZMPSTE24 recruit the UPS-dependent protein quality control machinery, an issue not well understood for any multispanning membrane protein. Our humanized yeast assay will also facilitate dissection of the prelamin A substrate to define a ZMPSTE24 consensus cleavage sequence and to probe the role of farnesyl for ZMPSTE24-mediated cleavage. Ultimately the capacity to perform deep mutational scanning followed by specific screens and selections in yeast (66,67) will facilitate isolation of separation-of-function alleles, in which ZMPSTE24 residues specific for prelamin A processing, declogging, and antiviral activity can be identified.

MATERIALS AND METHODS

Plasmids and strains used in this study

Plasmids used in this study are listed in Table 3. All plasmids were constructed using standard molecular biology techniques, including NEBuilder HiFi Assembly (New England Biolabs) and Quickchange mutagenesis (Stratagene). When mutating *ZMPSTE24*-containing plasmids, *E. coli* competent cells (Stbl2; Invitrogen) were transformed and grown at 30°C. ZMPSTE24 plasmids are *CEN*/*URA3* containing N-terminally-$His_{10}HA_3$-tagged human *ZMPSTE24* expressed from the *PGK1* promoter. Plasmid pSM3094 was constructed by subcloning a *Sac*II-*Xho*I fragment containing N-terminally-$His_{10}HA_3$-tagged yeast *STE24* from pSM1282 (68) into the same sites of pRS316. Plasmid pSM3283 is *CEN/HIS3* containing a single Flag-epitope at the N-terminus of ZMPSTE24 expressed from the *PGK1* promoter.

Plasmid pSM3173 is an integrating vector derived from Kp173 (a generous gift of Rong Li, JHU School of Medicine). Briefly, PCR-generated fragments from the *PRC1* promoter (-800 to -1), His_{10}-myc_3 and human *LMNA* (corresponding to amino acids 431-664) were recombined *in vitro* with a PCR-generated gapped Kp173 using NEB HiFi Assembly. Plasmids pSM3177 (L647R) and pSM3360 (C661S) were generated with mutagenic oligos and Quickchange mutagenesis using pSM3173 as template. Plasmid pSM3178 that expresses mature lamin A was constructed by placing a stop codon after amino acid Y646 using NEB HiFi Assembly. All manipulations with *LMNA* sequences used DH5a or NEB5 cells (NEB) for propagation. All integrating vectors in this study recombine at the *TRP1* locus by selecting with nourseothricin (Nat). Plasmid sequences and maps available upon request.

Yeast strains used are listed in Table 4. To integrate *LMNA* constructs, integrating plasmids were linearized by *Eco*RV digestion and transformed into *ste24*Δ (SM4826) cells by standard yeast lithium acetate protocols. Transformants were selected on YPD containing 100 mg/ml nourseothricin. To generate the double mutants *ste24*Δ*doa10*Δ and *ste24*Δ*ste14*Δ, diploids were made by crossing single mutant strains of opposite mating types and the double mutants identified following sporulation and tetrad dissection. Strain SM6117 (*ste24*Δ P_{GAL1}-*PDI1-DHFR-Nglyc-3HA* (clogger) was used previously (43). ZMPSTE24-expressing plasmids were transformed into strains and selected on minimal SC-Ura or SC-Ura-His plates.

Yeast prelamin A cleavage assay

Typically, strains grown overnight in minimal medium (0.67% yeast nitrogen base, 0.5% ammonium sulfate, 2% glucose, supplemented with appropriate amino acids and supplements) were back diluted in fresh medium for 4-6 hours. Cells (1.5-2 $O.D._{600}$ cell equivalents) were pelleted, washed in water and lysed using NaOH pre-treatment and SDS protein sample buffer (69) at 65°C for 10-15 min. For analysis, lysates were centrifuged at 21k x g for 2 min, and the supernatant (0.3 OD cell equivalents per lane) were resolved on 10% SDS-polyacrylamide gels. Proteins were transferred to nitrocellulose (Bio-Rad Transblot Turbo), and the membrane was blocked using Western Blocking Reagent (Roche). Lamin proteins were detected using mouse anti-myc antibodies (4A6, Millipore) decorated with goat anti-mouse secondary IRDye 680RD antibodies (LI-COR) . Blots were re-probed using rat anti-HA (3F10, Roche) and rabbit anti-Sec61 (a generous gift of Dr. Randy Schekman, UC, Berkeley), and visualized using goat anti-rat IRDye 680RD and goat anti-rabbit IRDye 800CW secondary antibodies (LI-COR). Prelamin A cleavage was calculated using ImageStudio Lite (LI-COR) by quantifying mature lamin A signal compared to total lamin A signal (prelamin A + mature lamin A). ZMPSTE24 protein levels were quantified by measuring the HA signal to Sec61 signal.

Clogger assay

Translocon clogging was examined essentially as previously described (43). Strain SM6117 transformed with vector or ZMPSTE24-expressing plasmids were grown overnight in SC-Ura with 2% sucrose as the carbon source. Strains were back diluted in the same medium for 3 hours, and then induced by adding galactose to 2.5% for six hours prior to collecting cells. SDS-PAGE, western transfer and blocking were done as described for prelamin A cleavage. Clogger protein was detected using rat anti-HA (3F10, Roche) and LI-COR secondary antibodies. Inserted, and clogged/cytoplasmic forms were quantified using ImageStudio Lite (LI-COR).

Proteasome inhibition

To test the effect of proteasome inhibition on ZMPSTE24 protein levels and prelamin A cleavage, strain SM6159 (*ste24*Δ*pdr5*Δ P_{PRC1}*-10His-3myc-LMNA*$_{CT}$) transformed with the indicated ZMPSTE24 alleles were grown to log phase in SC-Ura medium, and treated with either DMSO or 100 mM Bortezomib (from 30mM stock in DMSO) for 1 hr at 30°C. The *pdr5*Δ mutation was introduced to enhance the efficacy of drug treatment as previously described (70,71). Detergent extracts, SDS-PAGE, and western blotting were done as described above.

ACKNOWLEDGMENTS

This work was funded by grants R01 GM041223 (to SM) and R01 GM106082 (to CAH) from the National Institutes of Health. EPC and LN are funded for this work by UK Medical Research Council grant number MR/L017458/1. EPC is also funded by the Structural Genomics Consortium (SGC), which is a registered charity (number 1097737) that receives funds from AbbVie, Bayer Pharma AG, Boehringer Ingelheim, the Canada Foundation for Innovation, Genome Canada, GlaxoSmithKline, Janssen, Lilly Canada, Merck & Co., the Novartis Research Foundation, the Ontario Ministry of Economic Development and Innovation, Pfizer, São Paulo Research Foundation-FAPESP, Takeda, EU/EFPIA Innovative Medicines Initiative (IMI) Joint Undertaking (ULTRA-DD grant n° 115766) and the Wellcome Trust [092809/Z/10/Z].

TABLES

Table 1. ZMPSTE24 missense mutations that result in MAD-B or atypical progeria

Partial *zmpste24 mutation*	Partial/Null *zmpste24* mutation	Disease	Accumulates prelamin A	ZMPSTE24 levels	References
L94P	L94P	MAD-B	Yes	Decreased	(52)
P248L	Q41X	MAD-B	Yes	ND	(72) (54)
P248L	W450X	MAD-B	Yes	ND	(73) (72)
N265S	Y70S(fsX3)	MAD-B	ND	ND	(74)
N265S	L362F(fsX18)	AT "HGPS"	Yes	ND	(55)
N265S	L362F(fsX18)	MAD-B	ND	ND	Agarwal et al, 2006
W340R	L362F(fsX18)	MAD-B	ND	ND	(25) (22)
Y399C	Y399C *(LOH)	MAD-B	ND	ND	(75)
L425P	L425P	MAD-B	Yes	ND	(53)
L438F	none detected	Metabolic syndrome	Yes	Normal	(27) (28)
L438F	none detected	Nonalchoholic fatty liver disease (NAFLD)	ND	ND	(26)
L462R	none detected	RD	ND	ND	(62)

*LOH is loss of heterozygosity

Table 2. ZMPSTE24 *in vivo* relative cleavage activity, steady state protein levels, and adjusted ZMPSTE24 enzyme activity (normalized to protein amount)

ZMPSTE24	Activity (% of WT)	Protein levels (% of WT)	Adjusted ZMPSTE24 activity (%)*	Mutant Class**
vector	1.2	0	NA	-
WT	100	100	100	N/A
L94P	11.3	34.1	33.1	Class III
P248L	20.5	13.8	148.6	Class II
N265S	26.2	84.3	31.1	Class I
H335A	1.5	70.0	2.1	N/A
H339A	1.9	72.0	2.6	N/A
W340R	41.7	39.6	105.3	Class II
Y399C	25.8	92.9	27.8	Class I
L425P	41.9	62.1	67.5	Class III
L438F	57.2	67.9	84.2	Class III
L462R	6.5	29.7	21.9	Class III

* Adjusted ZMPSTE24 activity = Activity/Protein levels X 100

** Class I disease mutants are affected mainly in enzymatic function, Class II mainly in protein stability, Class III I both

*** Catalytic dead mutants are in red

Table 3. Plasmids used in this study

Plasmid	Description	Reference
pSM171	pRS313 (CEN, *HIS3*)	(76)
pSM174	pRS316 (CEN, *URA3*)	(76)
pSM2671	pRS316::P_{PGK1}-*10His-3HA-zmpste24N265A*	(20)
pSM2672	pRS316::P_{PGK1}-*10His-3HA-zmpste24W340R*	(20)
pSM2673	pRS316::P_{PGK1}-*10His-3HA-zmpste24H335A*	(20)
pSM2676	pRS316::P_{PGK1}-*10His-3HA-zmpste24P248L*	(20)
pSM2677	pRS316::P_{PGK1}-*10His-3HA-ZMPSTE24*	(20)
pSM2982	pRS316::P_{PGK1}-*10His-3HA-zmpste24L94P*	(20)
pSM2984	pRS316::P_{PGK1}-*10His-3HA-zmpste24L438F*	(20)
pSM3094	pRS316::P_{PGK1}-*10His-3HA-STE24*	This study
pSM3162	pRS316::P_{PGK1}-*10His-3HA-zmpste24H339A*	This study
pSM3185	pRS316::P_{PGK1}-*10His-3HA-zmpste24L425P*	This study
pSM3186	pRS316::P_{PGK1}-*10His-3HA-zmpste24Y399C*	This study
pSM3283	pRS313::P_{PGK1}-*Flag-ZMPSTE24*	This study
pSM3317	pRS316::P_{PGK1}-*10His-3HA-zmpste24L462R*	This study
pSM3173	YIP-TRP1::NatMX-P_{PRC1}-*10His-3myc-LMNA(431-664)*	This study
pSM3177	YIP-TRP1::NatMX-P_{PRC1}-*10His-3myc-LMNA(431-664, L647R)*	This study
pSM3178	YIP-TRP1::NatMX-P_{PRC1}-*10His-3myc-LMNA(431-646)*	This study
pSM3360	YIP-TRP1::NatMX-P_{PRC1}-*10His-3myc-LMNA(431-664, C661S)*	This study

Table 4. Yeast strains used in this study

Strain	Genotype	Reference
SM4826	*ste24::KanMX met15Δ0 his3Δ1 leu2Δ0 ura3Δ0* Mat**a**	Deletion collection
SM6117	*ste24::Hyg^r HO::P$_{GAL1}$-PDI1-clogger-3HA met15Δ0 his3Δ1 leu2Δ0 ura3Δ0 Mat***a**	(43)
SM6158	*ste24::KanMX met15Δ0 his3Δ1 leu2Δ0 ura3Δ0 Mata TRP1::NatMX-P$_{PRC1}$-10His-3myc-LMNA(431-664) Mat***a**	This study
SM6159	*ste24::Hyg^r pdr5::KanMX met15Δ0 his3Δ1 leu2Δ0 ura3Δ0 TRP1::NatMX-P$_{PRC1}$-10His-3myc-LMNA(431-664) Mat***a**	This study
SM6173	*ste24::KanMX met15Δ0 his3Δ1 leu2Δ0 ura3Δ0 Mat***a** *TRP1::NatMX-P$_{PRC1}$-10His-3myc-LMNA(431-664, C661S) Mat***a**	This study
SM6177	*ste24::KanMXmet15Δ0 his3Δ1 leu2Δ0 ura3Δ0 Mata TRP1::NatMX-P$_{PRC1}$-10His-3myc-LMNA(431-664, L647R) Mat***a**	This study
SM6178	*ste24::KanMX met15Δ0 his3Δ1 leu2Δ0 ura3Δ0 Mata TRP1::NatMX-P$_{PRC1}$-10His-3myc-LMNA(431-646) Mat***a**	This study
SM6184	*ste24::KanMX doa10::KanMX met15Δ0 his3Δ1 leu2Δ0 ura3Δ0 Mata TRP1::NatMX-P$_{PRC1}$-10His-3myc-LMNA(431-664) Mat***a**	This study
SM6187	*ste24::KanMX ste14::KanMX lys2Δ0 his3Δ1 leu2Δ0 ura3Δ0 Mata TRP1::NatMX-P$_{PRC1}$-10His-3myc-LMNA(431-664) Mat*α	This study

FIGURE LEGENDS

Figure 1. The prelamin A biogenesis pathway. The four steps of prelamin A posttranslational processing shown here are described in the text. The lipid farnesyl (a 15-carbon-long isoprenoid lipid) and the carboxyl methyl group ($O\text{-}CH_3$) are indicated. The enzymes that mediate CAAX processing are shown: farnesyltransferase (FTase), the proteases ZMPSTE24 and Ras converting enzyme (RCE1), and the isoprenylcysteine carboxylmethyl transferase (ICMT). It should be noted that while Step 2 in CAAX processing can be carried out redundantly for prelamin A either by ZMPSTE24 or RCE1, Step 4 of prelamin A processing is solely mediated by ZMPSTE24. When ZMPSTE24 is absent, processing is blocked at Step 4 and not Step 2, since RCE1 is present.

Figure 2. **Prelamin A is processed to mature lamin A by human ZMPSTE24 in yeast.** (A) A schematic of the humanized yeast system is shown. The prelamin A model substrate contains amino acids 431-664 from the C-terminus of human *LMNA* (referred to $LMNA_{CT}$) fused to a 10His-3myc epitope tag. It is expressed from the *PRC1* promoter (P_{PRC1}) and is chromosomally integrated into a *ste24*Δ strain background, resulting in strain SM6158. Full-length human ZMPSTE24 with an N-terminal 10His-3HA epitope tag is expressed from the *PGK1* promoter (P_{PGK1}) on a *CEN URA3* plasmid (pSM2677; (20)). (B) Lysates from *ste24*Δ strains expressing wild-type prelamin A (Lanes 1 and 2), uncleavable prelamin A (Lane 3, L647R) or mature lamin A (Lane 4, MAT) and human ZMPSTE24 (Lanes 1, 3 and 4) or vector alone (Lane 2) were analyzed for prelamin A processing by SDS-PAGE and western blotting with α-myc antibodies. Prelamin A (preLA) and mature lamin A (mLA) are indicated. Strains in lanes 1-4 are SM6158/pSM2677, SM6158/pRS316, SM6177/pSM2677, and SM6178/pSM2677, respectively.

Figure 3. Cleavage of prelamin A in yeast, as in mammalian cells, requires farnesylation of the CAAX motif and is diminished when carboxyl methylation is lacking. (A) Prelamin A processing is blocked when farnesylation is absent. Prelamin A processing in *ste24*Δ strains expressing the indicated $LMNA_{CT}$ (WT or C661S) and *ZMPSTE24* (WT and H335A) alleles was analyzed by SDS-PAGE and western blotting, as in Fig. 2. (B) The efficiency of prelamin A processing is reduced in a *ste14*Δ mutant strain. Prelamin A processing in strains expressing the indicated *ZMPSTE24* alleles was analyzed. Strains are *ste24*Δ only (Lanes 1 and 2) or a *ste24*Δ*ste14*Δ double mutant (Lane 3). Strains in lanes 1-3 are SM6158/pSM2677, SM6158/pSM2673, and SM6187/pSM2677, respectively.

Figure 4. ZMPSTE24 disease mutants show diminished prelamin A cleavage, and for some alleles dramatically decreased protein levels. Lysates from strain SM6158 (*ste24*Δ *myc-*$LMNA_{CT}$) transformed with plasmids expressing the indicated HA-ZMPSTE24 alleles or vector only

were analyzed by SDS-PAGE and western blotting. (A) Average percentage of prelamin A cleavage for each ZMPSTE24 variant was calculated from 4 independent experiments, with standard deviation of the mean shown as error bars. For comparison, WT ZMPSTE24 cleavage was set to 100%. (B) The ZMPSTE24 protein was detected with α-HA antibodies, and the ZMPSTE24 levels were normalized to the loading control Sec61, with WT ZMPSTE24 set to 100%. The average and standard deviation of the mean are shown for the same 4 experiments as in (A).

Figure 5. Deletion of the ubiquitin ligase Doa10 stabilizes the unstable ZMPSTE24 variants, and enhances prelamin A cleavage for some, but not all mutants. Strains SM6158 (*ste24*Δ *myc-LMNA*$_{CT}$) or SM6184 (*ste24*Δ*doa10*Δ *myc-LMNA*$_{CT}$) expressing the indicated ZMPSTE24 variant were analyzed by SDS-PAGE and western blotting using α-HA (A) and α-myc (B) antibodies. ZMPSTE24 protein levels were normalized against the loading control Sec61 (not shown). The *doa10*Δ mutant strain is designated as "Δ" and the wild-type DOA10 strain as "+".. Data shown is average and standard deviation of the mean for four independent experiments.

Figure 6. Comparison of ZMPSTE24 mutants for clearance of the "clogger" protein. To examine the capacity of ZMPSTE24 mutants to promote clearance of a protein designed to clog the Sec61 translocon, strain SM6117 (*ste24*Δ P_{GAL}*-Clogger-HA*) transformed with the indicated ZMPSTE24 plasmids was induced to express the clogger protein by addition of galactose, as described in Materials and Methods. Lysates were resolved by SDS-PAGE and probed with α-HA antibodies to detect the clogger. The inserted and clogged or cytoplasmic species are indicated, with the percentage clogged/cytoplasmic graphed on the y-axis. Data shown is the average and standard error of the mean for five individual experiments.

Figure 7. Location of missense disease alleles in the ZMPSTE24 structure. Positions of missense disease alleles in Table 1 are indicated on a ribbon diagram of the ZMPSTE24 structure (PDB entry 2YPT (32)). Yellow ball is zinc at the catalytic site.

SUPPLEMENTARY FIGURE LEGENDS

Figure S1. **Yeast Ste24 can catalyze prelamin A processing as efficiently as human ZMPSTE24**. Lysates were prepared from SM6158 (*ste24*Δ *myc-LMNA*$_{CT}$) cells transformed with vector only (Lane 1), pSM2677 (human *ZMPSTE24*, Lane 2) or pSM3094 (yeast *STE24*, Lane 3) and subjected to SDS-PAGE and Western blotting with α-*myc* antibodies to detect processing of prelamin A and α-HA antibodies to detect the ZMPSTE24 or Ste24 proteins, which both contain an N-terminal 10His-3HA epitope tag and are expressed from the same promoter. Although similar in size, ZMPSTE24 (475 amino acids) and Ste24 (453 amino acids) migrate significantly different by SDS-PAGE.

Figure S2. The extent of prelamin A processing depends on the amount of ZMPSTE24 cells express. Lysates were prepared from strain SM6158 (*ste24*Δ *myc-LMNA*$_{CT}$) containing empty vectors only (pRS313 and pRS316; Lane 1), HA-ZMPSTE24 and empty vector (pSM2677 and pRS313; Lane 2), Flag-ZMPSTE24 and empty vector (pSM3283 and pRS316; Lane 3) or HA-ZMPSTE24 and Flag-ZMPSTE24 (pSM2677 and pSM3283; Lane 4) and were analyzed by western blotting as described. Prelamin A cleavage is expressed as an average from three independent trials and standard deviation of the mean is indicated. With a single copy of *ZMPSTE24* expressed from the *PGK1* promoter, the prelamin A model substrate undergoes 65-80% processing (lanes 2 and 3), which increased to 90% with two copies (lane 4). It is possible that 100% processing cannot be achieved because a small percentage of prelamin A is not farnesylated.

Figure S3. Treatment of cells with the proteasome inhibitor Bortezomib improves the protein level for unstable ZMPSTE24 variants, but does not enhance prelamin A cleavage. SM6159 (*ste24*Δ*pdr5*Δ *myc-LMNA*$_{CT}$) transformed with the indicated ZMPSTE24 variants were treated with DMSO or Bortezomib **(**Btz;100 μM) for 1hr at 30°C and extracts were subjected to SDS-PAGE and western blotting. A) ZMPSTE24 protein level; B) Prelamin A cleavage. Data shown is the average and standard deviation of the mean for three independent experiments.

Figure S4. **ZMPSTE24 disease alleles do not exhibit dominance in the yeast prelamin A cleavage assay.** Strain SM6158 (*ste24*Δ *myc-LMNA*$_{CT}$) transformed with the indicated HA-ZMPSTE24 disease alleles and either pRS313 (vector only; -) or pSM3283 (which expresses WT Flag-ZMPSTE24; +) were assayed for *in vivo* prelamin A cleavage. Lysates were resolved by SDS-PAGE and proteins detected by immunoblotting against myc (prelamin A), HA (HA-ZMPSTE24) and Flag (Flag-ZMPSTE24). So long as at least one ZMPSTE24 allele is WT (lanes 2,

4 and 6) processing of prelamin A is close to 70%, even if a mutant allele is present.

REFERENCES

1. Bergo, M. O., Gavino, B., Ross, J., Schmidt, W. K., Hong, C., Kendall, L. V., Mohr, A., Meta, M., Genant, H., Jiang, Y., Wisner, E. R., Van Bruggen, N., Carano, R. A., Michaelis, S., Griffey, S. M., and Young, S. G. (2002) Zmpste24 deficiency in mice causes spontaneous bone fractures, muscle weakness, and a prelamin A processing defect. *Proc Natl Acad Sci U S A* **99**, 13049-13054
2. Michaelis, S., and Hrycyna, C. A. (2013) Biochemistry. A protease for the ages. *Science* **339**, 1529-1530
3. Pendas, A. M., Zhou, Z., Cadinanos, J., Freije, J. M., Wang, J., Hultenby, K., Astudillo, A., Wernerson, A., Rodriguez, F., Tryggvason, K., and Lopez-Otin, C. (2002) Defective prelamin A processing and muscular and adipocyte alterations in Zmpste24 metalloproteinase-deficient mice. *Nat Genet* **31**, 94-99
4. Butin-Israeli, V., Adam, S. A., Goldman, A. E., and Goldman, R. D. (2012) Nuclear lamin functions and disease. *Trends Genet* **28**, 464-471
5. Dechat, T., Adam, S. A., Taimen, P., Shimi, T., and Goldman, R. D. (2010) Nuclear lamins. *Cold Spring Harb Perspect Biol* **2**, a000547
6. Dittmer, T. A., and Misteli, T. (2011) The lamin protein family. *Genome Biol* **12**, 222
7. Dorado, B., and Andres, V. (2017) A-type lamins and cardiovascular disease in premature aging syndromes. *Curr Opin Cell Biol* **46**, 17-25
8. Gerace, L., and Huber, M. D. (2012) Nuclear lamina at the crossroads of the cytoplasm and nucleus. *J Struct Biol* **177**, 24-31
9. Gruenbaum, Y., and Foisner, R. (2015) Lamins: nuclear intermediate filament proteins with fundamental functions in nuclear mechanics and genome regulation. *Annu Rev Biochem* **84**, 131-164
10. Mattout, A., Dechat, T., Adam, S. A., Goldman, R. D., and Gruenbaum, Y. (2006) Nuclear lamins, diseases and aging. *Curr Opin Cell Biol* **18**, 335-341
11. Capell, B. C., and Collins, F. S. (2006) Human laminopathies: nuclei gone genetically awry. *Nat Rev Genet* **7**, 940-952
12. Davies, B. S., Fong, L. G., Yang, S. H., Coffinier, C., and Young, S. G. (2009) The posttranslational processing of prelamin A and disease. *Annu Rev Genomics Hum Genet* **10**, 153-174
13. Gordon, L. B., Rothman, F. G., Lopez-Otin, C., and Misteli, T. (2014) Progeria: a paradigm for translational medicine. *Cell* **156**, 400-407
14. De Sandre-Giovannoli, A., Bernard, R., Cau, P., Navarro, C., Amiel, J., Boccaccio, I., Lyonnet, S., Stewart, C. L., Munnich, A., Le Merrer, M., and Levy, N. (2003) Lamin a truncation in Hutchinson-Gilford progeria. *Science* **300**, 2055
15. Eriksson, M., Brown, W. T., Gordon, L. B., Glynn, M. W., Singer, J., Scott, L., Erdos, M. R., Robbins, C. M., Moses, T. Y., Berglund, P., Dutra, A., Pak, E., Durkin, S., Csoka, A. B., Boehnke, M., Glover, T. W., and Collins, F. S. (2003) Recurrent de novo point mutations in lamin A cause Hutchinson-Gilford progeria syndrome. *Nature* **423**, 293-298
16. Navarro, C. L., Esteves-Vieira, V., Courrier, S., Boyer, A., Duong Nguyen, T., Huong le, T. T., Meinke, P., Schroder, W., Cormier-Daire, V., Sznajer, Y., Amor, D. J., Lagerstedt, K., Biervliet, M., van den Akker, P. C., Cau, P., Roll, P., Levy, N., Badens, C., Wehnert, M., and De Sandre-Giovannoli, A. (2014) New ZMPSTE24 (FACE1) mutations in patients affected

with restrictive dermopathy or related progeroid syndromes and mutation update. *Eur J Hum Genet* **22**, 1002-1011

17. Michaelis, S., and Barrowman, J. (2012) Biogenesis of the *Saccharomyces cerevisiae* pheromone a-factor, from yeast mating to human disease. *Microbiol Mol Biol Rev* **76**, 626-651
18. Wang, M., and Casey, P. J. (2016) Protein prenylation: unique fats make their mark on biology. *Nat Rev Mol Cell Biol* **17**, 110-122
19. Worman, H. J., Fong, L. G., Muchir, A., and Young, S. G. (2009) Laminopathies and the long strange trip from basic cell biology to therapy. *J Clin Invest* **119**, 1825-1836
20. Barrowman, J., Wiley, P. A., Hudon-Miller, S. E., Hrycyna, C. A., and Michaelis, S. (2012) Human ZMPSTE24 disease mutations: residual proteolytic activity correlates with disease severity. *Hum Mol Genet* **21**, 4084-4093
21. Merideth, M. A., Gordon, L. B., Clauss, S., Sachdev, V., Smith, A. C., Perry, M. B., Brewer, C. C., Zalewski, C., Kim, H. J., Solomon, B., Brooks, B. P., Gerber, L. H., Turner, M. L., Domingo, D. L., Hart, T. C., Graf, J., Reynolds, J. C., Gropman, A., Yanovski, J. A., Gerhard-Herman, M., Collins, F. S., Nabel, E. G., Cannon, R. O., 3rd, Gahl, W. A., and Introne, W. J. (2008) Phenotype and course of Hutchinson-Gilford progeria syndrome. *N Engl J Med* **358**, 592-604
22. Moulson, C. L., Go, G., Gardner, J. M., van der Wal, A. C., Smitt, J. H., van Hagen, J. M., and Miner, J. H. (2005) Homozygous and compound heterozygous mutations in ZMPSTE24 cause the laminopathy restrictive dermopathy. *J Invest Dermatol* **125**, 913-919
23. Navarro, C. L., Cadinanos, J., De Sandre-Giovannoli, A., Bernard, R., Courrier, S., Boccaccio, I., Boyer, A., Kleijer, W. J., Wagner, A., Giuliano, F., Beemer, F. A., Freije, J. M., Cau, P., Hennekam, R. C., Lopez-Otin, C., Badens, C., and Levy, N. (2005) Loss of ZMPSTE24 (FACE-1) causes autosomal recessive restrictive dermopathy and accumulation of Lamin A precursors. *Hum Mol Genet* **14**, 1503-1513
24. Smigiel, R., Jakubiak, A., Esteves-Vieira, V., Szela, K., Halon, A., Jurek, T., Levy, N., and De Sandre-Giovannoli, A. (2010) Novel frameshifting mutations of the ZMPSTE24 gene in two siblings affected with restrictive dermopathy and review of the mutations described in the literature. *Am J Med Genet A* **152A**, 447-452
25. Agarwal, A. K., Fryns, J. P., Auchus, R. J., and Garg, A. (2003) Zinc metalloproteinase, ZMPSTE24, is mutated in mandibuloacral dysplasia. *Hum Mol Genet* **12**, 1995-2001
26. Brady, G. F., Kwan, R., Ulintz, P. J., Nguyen, P., Bassirian, S., Basrur, V., Nesvizhskii, A. I., Loomba, R., and Omary, M. B. (2017) Nuclear lamina genetic variants, including a truncated LAP2, in twins and siblings with nonalcoholic fatty liver disease. *Hepatology*
27. Dutour, A., Roll, P., Gaborit, B., Courrier, S., Alessi, M. C., Tregouet, D. A., Angelis, F., Robaglia-Schlupp, A., Lesavre, N., Cau, P., Levy, N., Badens, C., and Morange, P. E. (2011) High prevalence of laminopathies among patients with metabolic syndrome. *Hum Mol Genet* **20**, 3779-3786
28. Galant, D., Gaborit, B., Desgrouas, C., Abdesselam, I., Bernard, M., Levy, N., Merono, F., Coirault, C., Roll, P., Lagarde, A., Bonello-Palot, N., Bourgeois, P., Dutour, A., and Badens, C. (2016) A Heterozygous ZMPSTE24 Mutation Associated with Severe Metabolic Syndrome, Ectopic Fat Accumulation, and Dilated Cardiomyopathy. *Cells* **5**
29. Ragnauth, C. D., Warren, D. T., Liu, Y., McNair, R., Tajsic, T., Figg, N., Shroff, R., Skepper, J., and Shanahan, C. M. (2010) Prelamin A acts to accelerate smooth muscle cell senescence and is a novel biomarker of human vascular aging. *Circulation* **121**, 2200-2210

30. Barrowman, J., and Michaelis, S. (2009) ZMPSTE24, an integral membrane zinc metalloprotease with a connection to progeroid disorders. *Biol Chem* **390**, 761-773

31. Pryor, E. E., Jr., Horanyi, P. S., Clark, K. M., Fedoriw, N., Connelly, S. M., Koszelak-Rosenblum, M., Zhu, G., Malkowski, M. G., Wiener, M. C., and Dumont, M. E. (2013) Structure of the integral membrane protein CAAX protease Ste24p. *Science* **339**, 1600-1604

32. Quigley, A., Dong, Y. Y., Pike, A. C., Dong, L., Shrestha, L., Berridge, G., Stansfeld, P. J., Sansom, M. S., Edwards, A. M., Bountra, C., von Delft, F., Bullock, A. N., Burgess-Brown, N. A., and Carpenter, E. P. (2013) The structural basis of ZMPSTE24-dependent laminopathies. *Science* **339**, 1604-1607

33. Barrowman, J., and Michaelis, S. (2011) CAAX Processing and Yeast a-Factor Biogenesis. *Enzymes* **30**, 13-41

34. Boyartchuk, V. L., and Rine, J. (1998) Roles of prenyl protein proteases in maturation of *Saccharomyces cerevisiae* a-factor. *Genetics* **150**, 95-101

35. Fujimura-Kamada, K., Nouvet, F. J., and Michaelis, S. (1997) A novel membrane-associated metalloprotease, Ste24p, is required for the first step of NH2-terminal processing of the yeast a-factor precursor. *J Cell Biol* **136**, 271-285

36. Tam, A., Nouvet, F. J., Fujimura-Kamada, K., Slunt, H., Sisodia, S. S., and Michaelis, S. (1998) Dual roles for Ste24p in yeast a-factor maturation: NH2-terminal proteolysis and COOH-terminal CAAX processing. *J Cell Biol* **142**, 635-649

37. Beck, L. A., Hosick, T. J., and Sinensky, M. (1990) Isoprenylation is required for the processing of the lamin A precursor. *J Cell Biol* **110**, 1489-1499

38. Sinensky, M., Fantle, K., Trujillo, M., McLain, T., Kupfer, A., and Dalton, M. (1994) The processing pathway of prelamin A. *J Cell Sci* **107 (Pt 1)**, 61-67

39. Clark, K. M., Jenkins, J. L., Fedoriw, N., and Dumont, M. E. (2017) Human CaaX protease ZMPSTE24 expressed in yeast: Structure and inhibition by HIV protease inhibitors. *Protein Sci* **26**, 242-257

40. Coffinier, C., Hudon, S. E., Farber, E. A., Chang, S. Y., Hrycyna, C. A., Young, S. G., and Fong, L. G. (2007) HIV protease inhibitors block the zinc metalloproteinase ZMPSTE24 and lead to an accumulation of prelamin A in cells. *Proc Natl Acad Sci U S A* **104**, 13432-13437

41. Mehmood, S., Marcoux, J., Gault, J., Quigley, A., Michaelis, S., Young, S. G., Carpenter, E. P., and Robinson, C. V. (2016) Mass spectrometry captures off-target drug binding and provides mechanistic insights into the human metalloprotease ZMPSTE24. *Nat Chem* **8**, 1152-1158

42. Barrowman, J., Hamblet, C., George, C. M., and Michaelis, S. (2008) Analysis of prelamin A biogenesis reveals the nucleus to be a CaaX processing compartment. *Mol Biol Cell* **19**, 5398-5408

43. Ast, T., Michaelis, S., and Schuldiner, M. (2016) The Protease Ste24 Clears Clogged Translocons. *Cell* **164**, 103-114

44. Fu, B., Wang, L., Li, S., and Dorf, M. E. (2017) ZMPSTE24 defends against influenza and other pathogenic viruses. *J Exp Med* **214**, 919-929

45. Schmidt, W. K., Tam, A., and Michaelis, S. (2000) Reconstitution of the Ste24p-dependent N-terminal proteolytic step in yeast a-factor biogenesis. *J Biol Chem* **275**, 6227-6233

46. Barrowman, J., Hamblet, C., Kane, M. S., and Michaelis, S. (2012) Requirements for efficient proteolytic cleavage of prelamin A by ZMPSTE24. *PLoS One* **7**, e32120

47. Hennekes, H., and Nigg, E. A. (1994) The role of isoprenylation in membrane attachment of nuclear lamins. A single point mutation prevents proteolytic cleavage of the lamin A precursor and confers membrane binding properties. *J Cell Sci* **107 (Pt 4)**, 1019-1029

48. Mallampalli, M. P., Huyer, G., Bendale, P., Gelb, M. H., and Michaelis, S. (2005) Inhibiting farnesylation reverses the nuclear morphology defect in a HeLa cell model for Hutchinson-Gilford progeria syndrome. *Proc Natl Acad Sci U S A* **102**, 14416-14421

49. Wang, Y., Lichter-Konecki, U., Anyane-Yeboa, K., Shaw, J. E., Lu, J. T., Ostlund, C., Shin, J. Y., Clark, L. N., Gundersen, G. G., Nagy, P. L., and Worman, H. J. (2016) A mutation abolishing the ZMPSTE24 cleavage site in prelamin A causes a progeroid disorder. *J Cell Sci* **129**, 1975-1980

50. Yang, S. H., Andres, D. A., Spielmann, H. P., Young, S. G., and Fong, L. G. (2008) Progerin elicits disease phenotypes of progeria in mice whether or not it is farnesylated. *J Clin Invest* **118**, 3291-3300

51. Young, S. G., Fong, L. G., and Michaelis, S. (2005) Prelamin A, Zmpste24, misshapen cell nuclei, and progeria--new evidence suggesting that protein farnesylation could be important for disease pathogenesis. *J Lipid Res* **46**, 2531-2558

52. Ben Yaou, R., Navarro, C., Quijano-Roy, S., Bertrand, A. T., Massart, C., De Sandre-Giovannoli, A., Cadinanos, J., Mamchaoui, K., Butler-Browne, G., Estournet, B., Richard, P., Barois, A., Levy, N., and Bonne, G. (2011) Type B mandibuloacral dysplasia with congenital myopathy due to homozygous ZMPSTE24 missense mutation. *Eur J Hum Genet* **19**, 647-654

53. Harhouri, K., Navarro, C., Baquerre, C., Da Silva, N., Bartoli, C., Casey, F., Mawuse, G. K., Doubaj, Y., Levy, N., and De Sandre-Giovannoli, A. (2016) Antisense-Based Progerin Downregulation in HGPS-Like Patients' Cells. *Cells* **5**

54. Miyoshi, Y., Akagi, M., Agarwal, A. K., Namba, N., Kato-Nishimura, K., Mohri, I., Yamagata, M., Nakajima, S., Mushiake, S., Shima, M., Auchus, R. J., Taniike, M., Garg, A., and Ozono, K. (2008) Severe mandibuloacral dysplasia caused by novel compound heterozygous ZMPSTE24 mutations in two Japanese siblings. *Clin Genet* **73**, 535-544

55. Shackleton, S., Smallwood, D. T., Clayton, P., Wilson, L. C., Agarwal, A. K., Garg, A., and Trembath, R. C. (2005) Compound heterozygous ZMPSTE24 mutations reduce prelamin A processing and result in a severe progeroid phenotype. *J Med Genet* **42**, e36

56. Amaral, M. D. (2015) Novel personalized therapies for cystic fibrosis: treating the basic defect in all patients. *J Intern Med* **277**, 155-166

57. Brodsky, J. L. (2012) Cleaning up: ER-associated degradation to the rescue. *Cell* **151**, 1163-1167

58. Guerriero, C. J., and Brodsky, J. L. (2012) The delicate balance between secreted protein folding and endoplasmic reticulum-associated degradation in human physiology. *Physiol Rev* **92**, 537-576

59. Ravid, T., Kreft, S. G., and Hochstrasser, M. (2006) Membrane and soluble substrates of the Doa10 ubiquitin ligase are degraded by distinct pathways. *EMBO J* **25**, 533-543

60. Swanson, R., Locher, M., and Hochstrasser, M. (2001) A conserved ubiquitin ligase of the nuclear envelope/endoplasmic reticulum that functions in both ER-associated and Matalpha2 repressor degradation. *Genes Dev* **15**, 2660-2674

61. Deng, M., and Hochstrasser, M. (2006) Spatially regulated ubiquitin ligation by an ER/nuclear membrane ligase. *Nature* **443**, 827-831

62. Thill, M., Nguyen, T. D., Wehnert, M., Fischer, D., Hausser, I., Braun, S., and Jackisch, C. (2008) Restrictive dermopathy: a rare laminopathy. *Arch Gynecol Obstet* **278**, 201-208

63. Gogala, M., Becker, T., Beatrix, B., Armache, J. P., Barrio-Garcia, C., Berninghausen, O., and Beckmann, R. (2014) Structures of the Sec61 complex engaged in nascent peptide translocation or membrane insertion. *Nature* **506**, 107-110

64. Li, L., Park, E., Ling, J., Ingram, J., Ploegh, H., and Rapoport, T. A. (2016) Crystal structure of a substrate-engaged SecY protein-translocation channel. *Nature* **531**, 395-399

65. Pfeffer, S., Burbaum, L., Unverdorben, P., Pech, M., Chen, Y., Zimmermann, R., Beckmann, R., and Forster, F. (2015) Structure of the native Sec61 protein-conducting channel. *Nat Commun* **6**, 8403

66. Fowler, D. M., Stephany, J. J., and Fields, S. (2014) Measuring the activity of protein variants on a large scale using deep mutational scanning. *Nat Protoc* **9**, 2267-2284

67. Starita, L. M., and Fields, S. (2015) Deep Mutational Scanning: A Highly Parallel Method to Measure the Effects of Mutation on Protein Function. *Cold Spring Harb Protoc* **2015**, 711-714

68. Tam, A., Schmidt, W. K., and Michaelis, S. (2001) The multispanning membrane protein Ste24p catalyzes CAAX proteolysis and NH2-terminal processing of the yeast a-factor precursor. *J Biol Chem* **276**, 46798-46806

69. Kushnirov, V. V. (2000) Rapid and reliable protein extraction from yeast. *Yeast* **16**, 857-860

70. Collins, G. A., Gomez, T. A., Deshaies, R. J., and Tansey, W. P. (2010) Combined chemical and genetic approach to inhibit proteolysis by the proteasome. *Yeast* **27**, 965-974

71. Sung, M. K., Reitsma, J. M., Sweredoski, M. J., Hess, S., and Deshaies, R. J. (2016) Ribosomal proteins produced in excess are degraded by the ubiquitin-proteasome system. *Mol Biol Cell* **27**, 2642-2652

72. Akinci, B., Sankella, S., Gilpin, C., Ozono, K., Garg, A., and Agarwal, A. K. (2017) Progeroid syndrome patients with ZMPSTE24 deficiency could benefit when treated with rapamycin and dimethylsulfoxide. *Cold Spring Harb Mol Case Stud* **3**, a001339

73. Ahmad, Z., Zackai, E., Medne, L., and Garg, A. (2010) Early onset mandibuloacral dysplasia due to compound heterozygous mutations in ZMPSTE24. *Am J Med Genet A* **152A**, 2703-2710

74. Cunningham, V. J., D'Apice, M. R., Licata, N., Novelli, G., and Cundy, T. (2010) Skeletal phenotype of mandibuloacral dysplasia associated with mutations in ZMPSTE24. *Bone* **47**, 591-597

75. Haye, D., Dridi, H., Levy, J., Lambert, V., Lambert, M., Agha, M., Adjimi, F., Kohlhase, J., Lipsker, D., and Verloes, A. (2016) Failure of ossification of the occipital bone in mandibuloacral dysplasia type B. *Am J Med Genet A* **170**, 2750-2755

76. Sikorski, R. S., and Hieter, P. (1989) A system of shuttle vectors and yeast host strains designed for efficient manipulation of DNA in *Saccharomyces cerevisiae*. *Genetics* **122**, 19-27

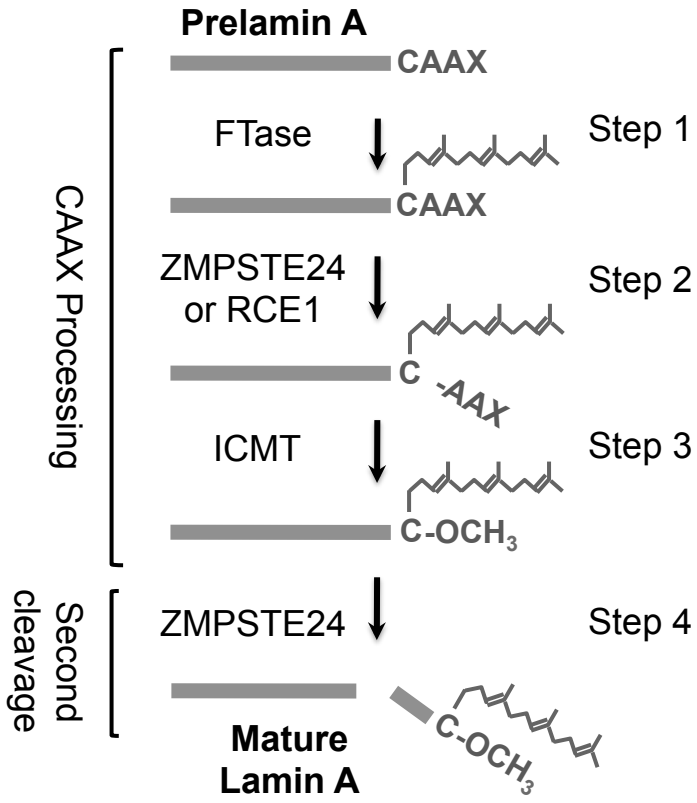

Figure 1. The prelamin A biogenesis pathway. The four steps of prelamin A posttranslational processing shown here are described in the text. The lipid farnesyl (a 15-carbon-long isoprenoid lipid) and the carboxyl methyl group (O-CH_3) are indicated. The enzymes that mediate CAAX processing are shown: farnesyltransferase (FTase), the proteases ZMPSTE24 and Ras converting enzyme (RCE1), and the isoprenylcysteine carboxylmethyl transferase (ICMT). It should be noted that while Step 2 in CAAX processing can be carried out redundantly for prelamin A either by ZMPSTE24 or RCE1, Step 4 of prelamin A processing is solely mediated by ZMPSTE24. When ZMPSTE24 is absent, processing is blocked at Step 4 and not Step 2, since RCE1 is present.

Figure 1

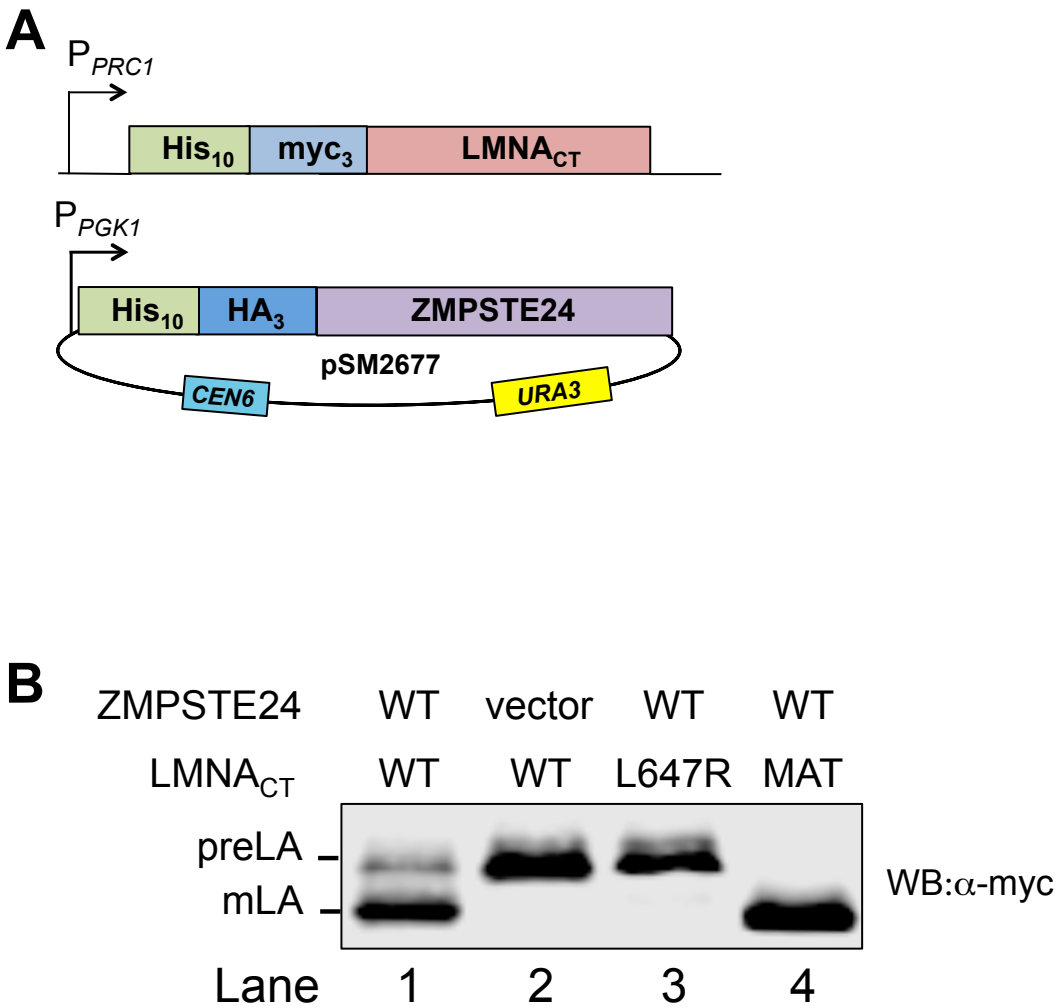

Figure 2. **Prelamin A is processed to mature lamin A by human ZMPSTE24 in yeast.** (A) A schematic of the humanized yeast system is shown. The prelamin A model substrate contains amino acids 431-664 from the C-terminus of human *LMNA* (referred to $LMNA_{CT}$) fused to a 10His-3myc epitope tag. It is expressed from the *PRC1* promoter (P_{PRC1}) and is chromosomally integrated into a *ste24*Δ strain background, resulting in strain SM6158. Full-length human ZMPSTE24 with an N-terminal 10His-3HA epitope tag is expressed from the *PGK1* promoter (P_{PGK1}) on a *CEN URA3* plasmid (pSM2677; (19)). (B) Lysates from *ste24*Δ strains expressing wild-type prelamin A (Lanes 1 and 2), uncleavable prelamin A (Lane 3, L647R) or mature lamin A (Lane 4, MAT) and human ZMPSTE24 (Lanes 1, 3 and 4) or vector alone (Lane 2) were analyzed for prelamin A processing by SDS-PAGE and western blotting with α-myc antibodies. Prelamin A (preLA) and mature lamin A (mLA) are indicated. Strains in lanes 1-4 are SM6158/pSM2677, SM6158/pRS316, SM6177/pSM2677, and SM6178/pSM2677, respectively.

Figure 2

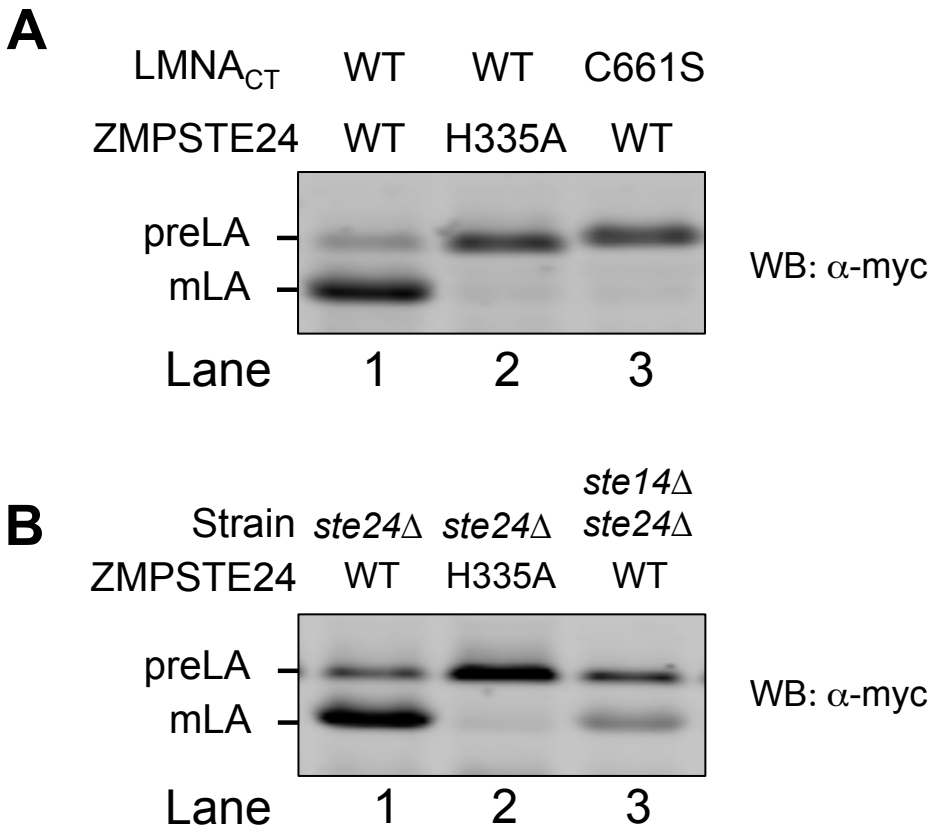

Figure 3. Cleavage of prelamin A in yeast, as in mammalian cells, requires farnesylation of the CAAX motif and is diminished when carboxyl methylation is lacking. (A) Prelamin A processing is blocked when farnesylation is absent. Prelamin A processing in *ste24*Δ strains expressing the indicated *LMNA*$_{CT}$ (WT or C661S) and *ZMPSTE24* (WT and H335A) alleles was analyzed by SDS-PAGE and western blotting, as in Fig. 2. (B) The efficiency of prelamin A processing is reduced in a *ste14*Δ mutant strain. Prelamin A processing in strains expressing the indicated *ZMPSTE24* alleles was analyzed. Strains are *ste24*Δ only (Lanes 1 and 2) or a *ste24*Δ*ste14*Δ double mutant (Lane 3). Strains in lanes 1-3 are SM6158/pSM2677, SM6158/pSM2673, and SM6187/pSM2677, respectively.

Figure 3

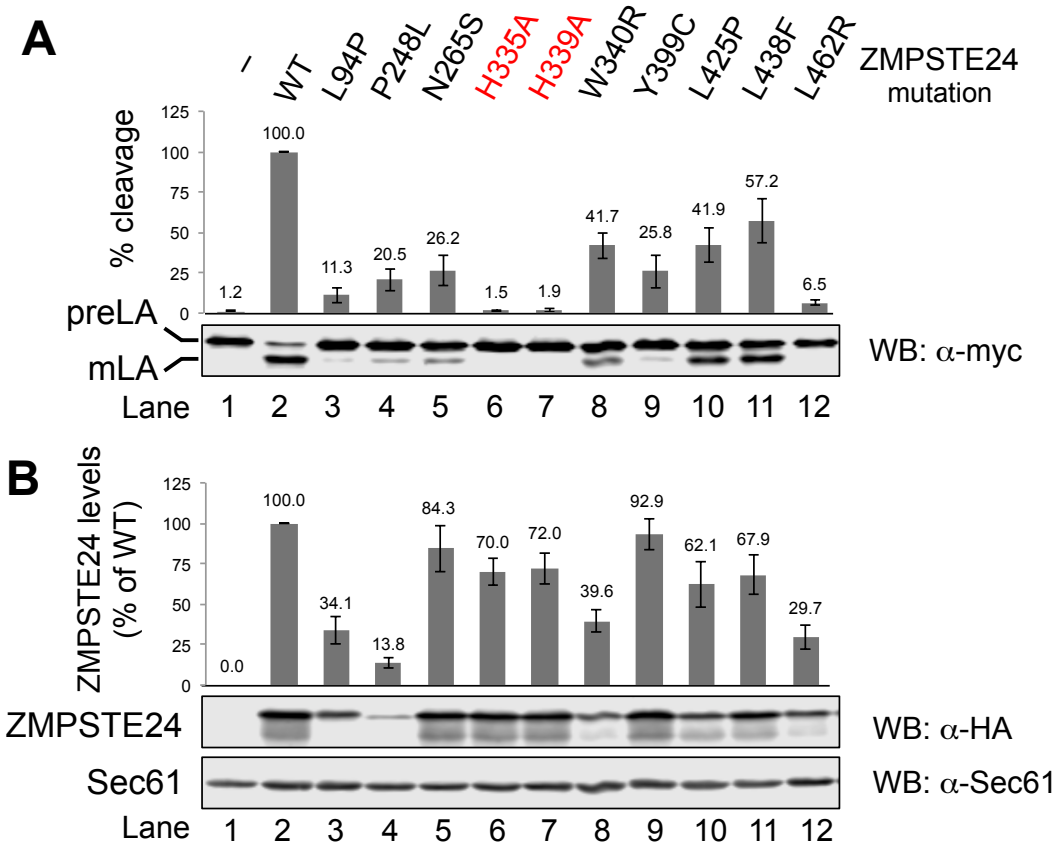

Figure 4. ZMPSTE24 disease mutants show diminished prelamin A cleavage, and for some alleles dramatically decreased protein levels. Lysates from strain SM6158 (*ste24Δ myc-LMNA$_{CT}$*) transformed with plasmids expressing the indicated HA-ZMPSTE24 alleles or vector only were analyzed by SDS-PAGE and western blotting. (A) Average percentage of prelamin A cleavage for each ZMPSTE24 variant was calculated from 4 independent experiments, with standard deviation of the mean shown as error bars. For comparison, WT ZMPSTE24 cleavage was set to 100%. (B) The ZMPSTE24 protein was detected with α-HA antibodies, and the ZMPSTE24 levels were normalized to the loading control Sec61, with WT ZMPSTE24 set to 100%. The average and standard deviation of the mean are shown for the same 4 experiments as in (A).

Figure 4

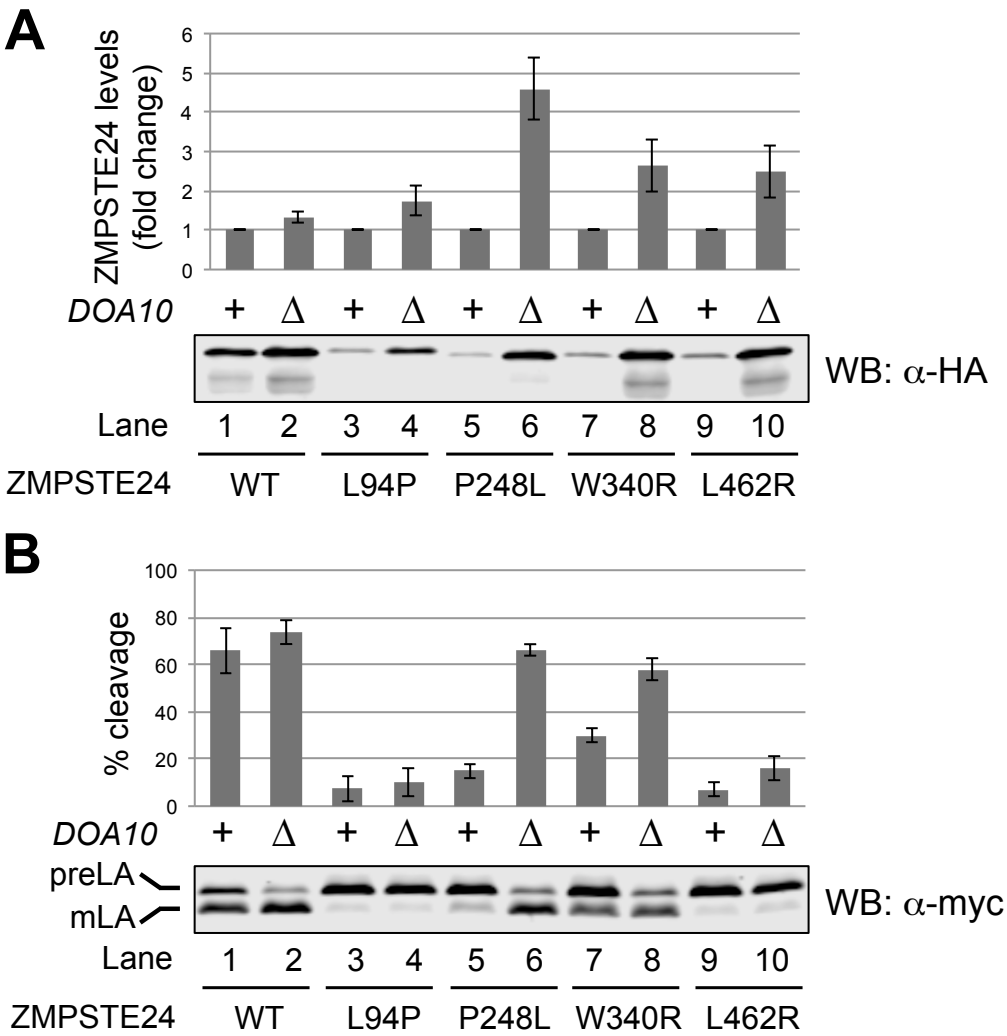

Figure 5. Deletion of the ubiquitin ligase Doa10 stabilizes the unstable ZMPSTE24 variants, and enhances prelamin A cleavage for some, but not all mutants. Strains SM6158 (*ste24Δ myc-LMNA*$_{CT}$) or SM6184 (*ste24Δdoa10Δ myc-LMNA*$_{CT}$) expressing the indicated ZMPSTE24 variant were analyzed by SDS-PAGE and western blotting using α-HA (A) and α-myc (B) antibodies. ZMPSTE24 protein levels were normalized against the loading control Sec61 (not shown). The *doa10Δ* mutant strain is designated as "Δ" and the wild-type DOA10 strain as "+". Data shown is average and standard deviation of the mean for four independent experiments.

Figure 5

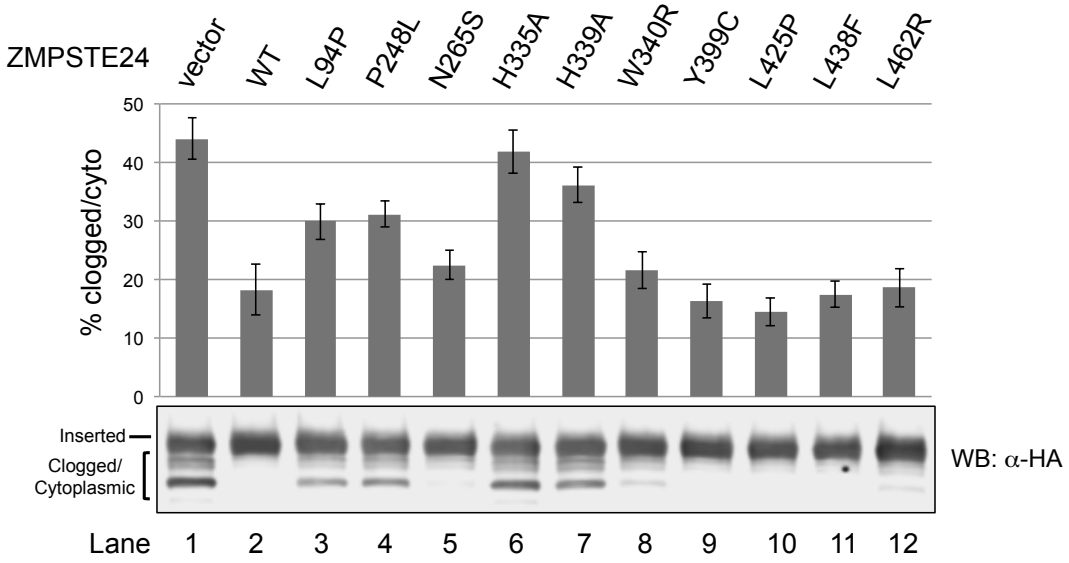

Figure 6. Comparison of ZMPSTE24 mutants for clearance of the "clogger" protein
To examine the capacity of ZMPSTE24 mutants to promote clearance of a protein designed to clog the Sec61 translocon, strain SM6117 (*ste24Δ* P_{GAL}*-Clogger-HA*) transformed with the indicated ZMPSTE24 plasmids was induced to express the clogger protein by addition of galactose, as described in Materials and Methods. Lysates were resolved by SDS-PAGE and probed with α-HA antibodies to detect the clogger. The inserted and clogged or cytoplasmic species are indicated, with the percentage clogged/cytoplasmic graphed on the y-axis. Data shown is the average and standard error of the mean for five individual experiments.

Figure 6

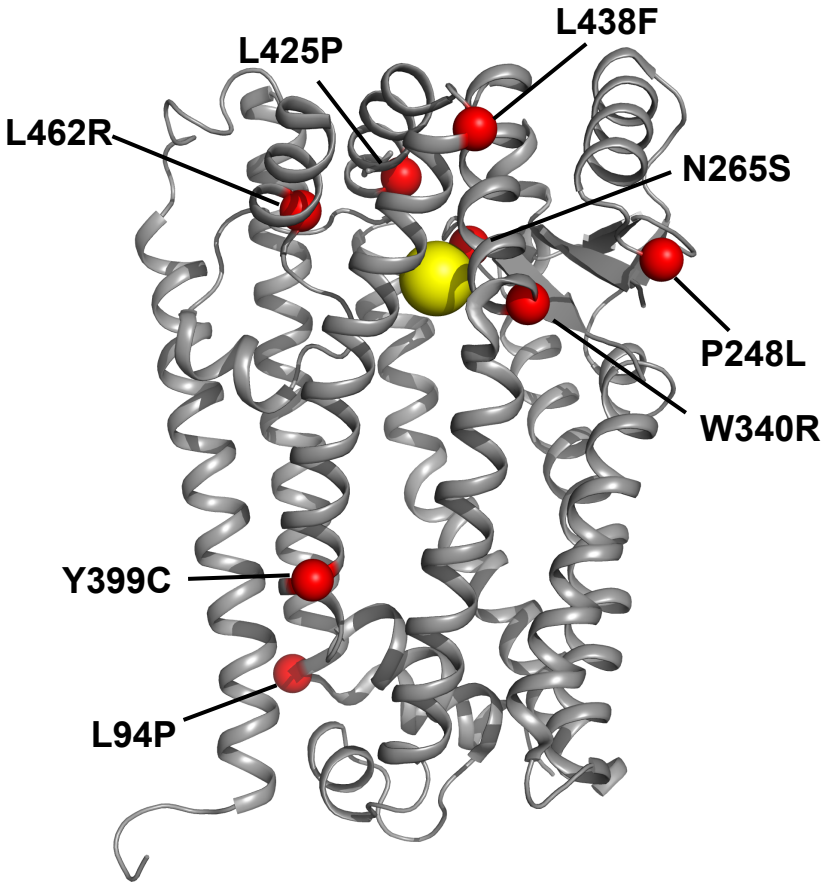

Figure 7. Location of missense disease alleles in the ZMPSTE24 structure. Positions of missense disease alleles in Table 1 are indicated on a ribbon diagram of the ZMPSTE24 structure (PDB entry 2YPT (31)). Yellow ball is zinc at the catalytic site.

Figure 7

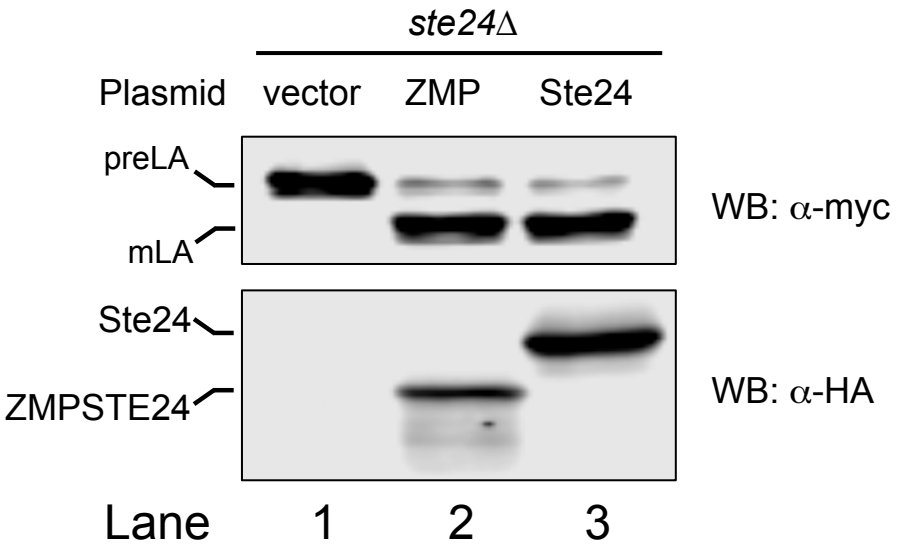

Figure S1. **Yeast Ste24 can catalyze prelamin A processing as efficiently as human ZMPSTE24**. Lysates were prepared from SM6158 (*ste24Δ myc-LMNA$_{CT}$*) cells transformed with vector only (Lane 1), pSM2677 (human *ZMPSTE24*, Lane 2) or pSM3094 (yeast *STE24*, Lane 3) and subjected to SDS-PAGE and Western blotting with α-*myc* antibodies to detect processing of prelamin A and α-HA antibodies to detect the ZMPSTE24 or Ste24 proteins, which both contain an N-terminal 10His-3HA epitope tag and are expressed from the same promoter. Although similar in size, ZMPSTE24 (475 amino acids) and Ste24 (453 amino acids) migrate significantly different by SDS-PAGE.

Figure S1

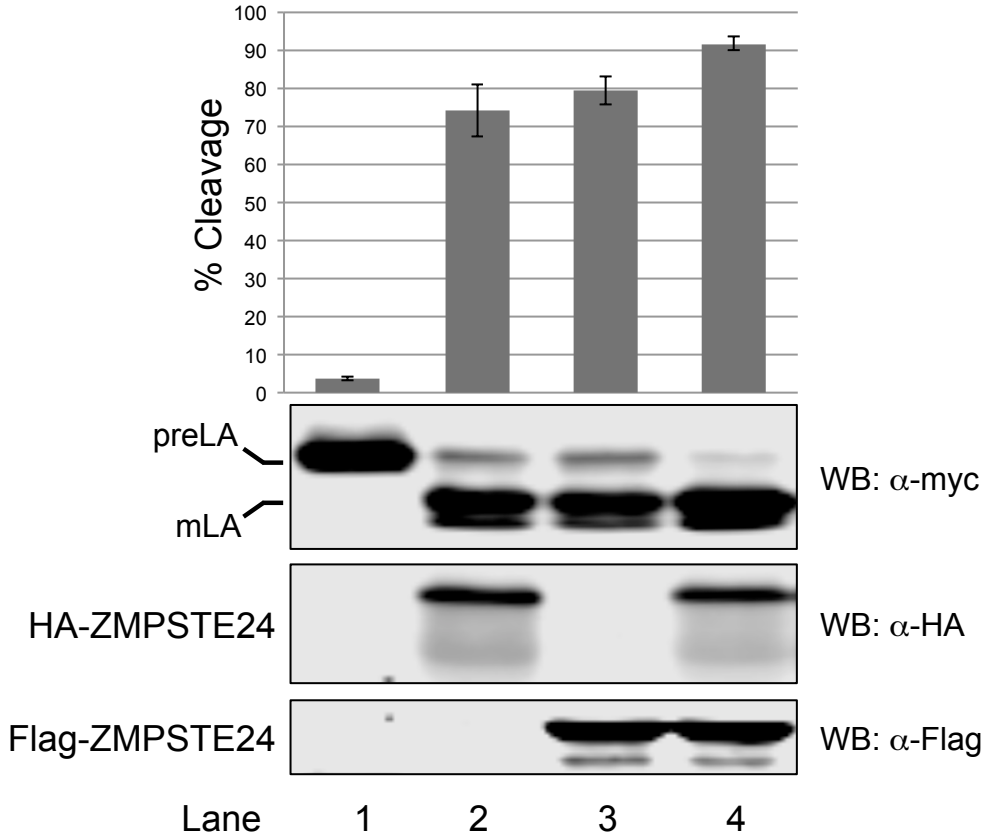

Figure S2. The extent of prelamin A processing depends on the amount of ZMPSTE24 cells express. Lysates were prepared from strain SM6158 (*ste24*Δ *myc-LMNA*$_{CT}$) containing empty vectors only (pRS313 and pRS316; Lane 1), HA-ZMPSTE24 and empty vector (pSM2677 and pRS313; Lane 2), Flag-ZMPSTE24 and empty vector (pSM3283 and pRS316; Lane 3) or HA-ZMPSTE24 and Flag-ZMPSTE24 (pSM2677 and pSM3283; Lane 4) and were analyzed by western blotting as described. Prelamin A cleavage is expressed as an average from three independent trials and standard deviation of the mean is indicated. With a single copy of *ZMPSTE24* expressed from the *PGK1* promoter, the prelamin A model substrate undergoes 70-80% processing (lanes 2 and 3), which increased to 90% with two copies (lane 4). It is possible that 100% processing cannot be achieved because a small percentage of prelamin A is not farnesylated.

Figure S2

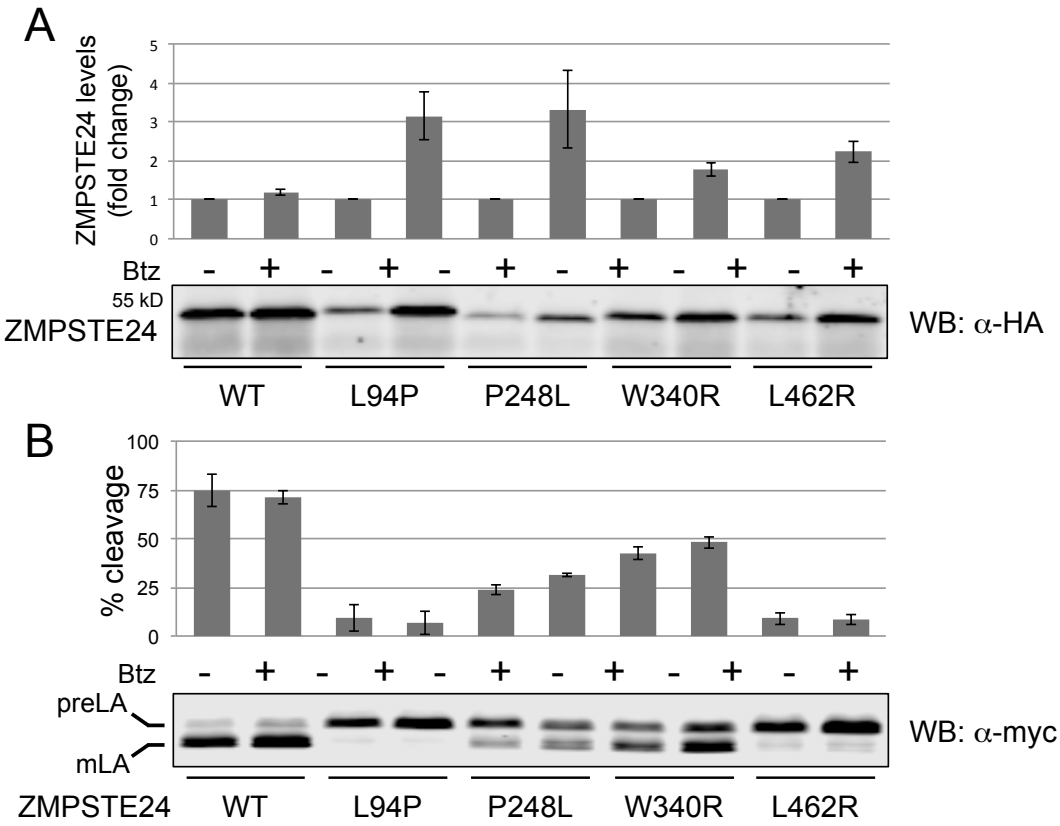

Figure S3. Treatment of cells with the proteasome inhibitor Bortezomib improves the protein level for unstable ZMPSTE24 variants, but does not enhance prelamin A cleavage. SM6159 (*ste24Δpdr5Δ myc-LMNA*$_{CT}$) transformed with the indicated ZMPSTE24 variants were treated with DMSO or Bortezomib (Btz;100 μM) for 1hr at 30°C and extracts were subjected to SDS-PAGE and western blotting. A) ZMPSTE24 protein level; B) Prelamin A cleavage. Data shown is the average and standard deviation of the mean for three independent experiments.

Figure S3

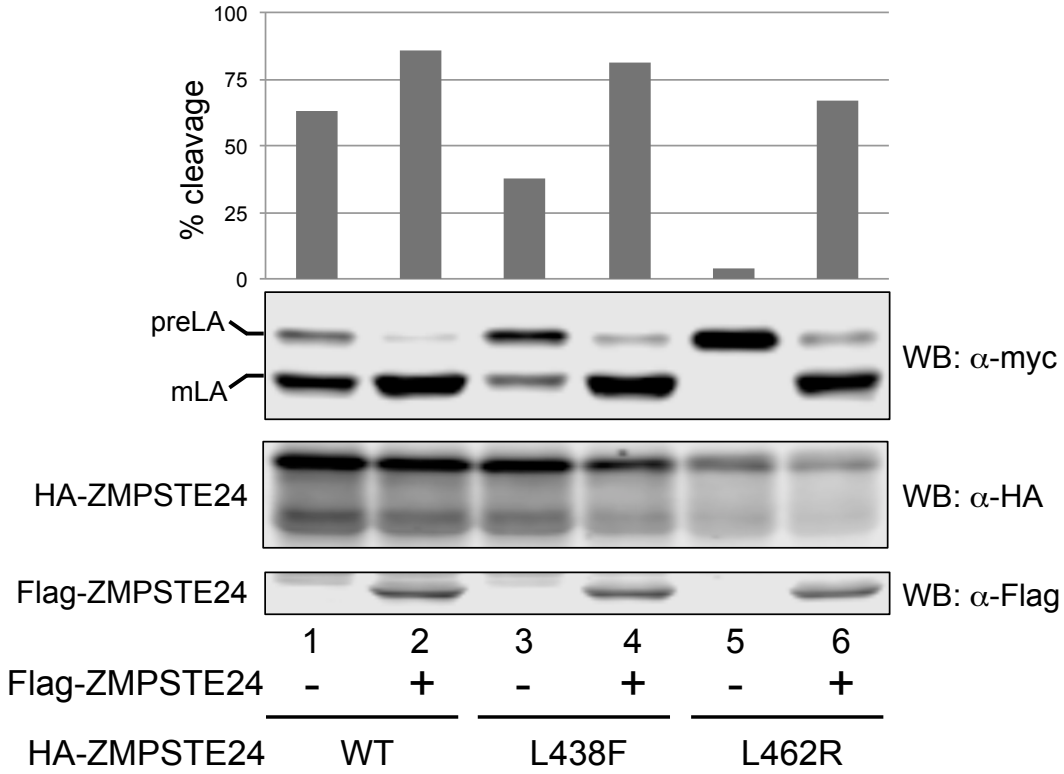

Figure S4. **ZMPSTE24 disease alleles do not exhibit dominance in the yeast prelamin A cleavage assay.** Strain SM6158 (*ste24Δ myc-LMNA$_{CT}$*) transformed with the indicated HA-ZMPSTE24 disease alleles and either pRS313 (vector only; -) or pSM3283 (which expresses WT Flag-ZMPSTE24; +) were assayed for *in vivo* prelamin A cleavage. Lysates were resolved by SDS-PAGE and proteins detected by immunoblotting against myc (prelamin A), HA (HA-ZMPSTE24) and Flag (Flag-ZMPSTE24). So long as at least one ZMPSTE24 allele is WT (lanes 2, 4 and 6) processing of prelamin A is close to 70%, even if a mutant allele is present.

Figure S4